3-26-2015

WiFi and LTE Coexistence in the Unlicensed Spectrum

Nadisanka Rupasinghe
Florida International University, rrupa001@fiu.edu

DOI: 10.25148/etd.FI15032155

FLORIDA INTERNATIONAL UNIVERSITY

Miami, Florida

WiFi AND LTE COEXISTENCE IN THE UNLICENSED SPECTRUM

A thesis submitted in partial fulfillment of

the requirements for the degree of

MASTER OF SCIENCE

in

ELECTRICAL AND COMPUTER ENGINEERING

by

R.A. Nadisanka Rupasinghe

2015

To: Dean Amir Mirmiran
College of Engineering and Computing

This thesis, written by R.A. Nadisanka Rupasinghe, and entitled WiFi and LTE Coexistence in the Unlicensed Spectrum, having been approved in respect to style and intellectual content, is referred to you for judgment.

We have read this thesis and recommend that it be approved.

Walid Saad

Hai Deng

Nazih Pala

İsmail Güvenç, Major Professor

Date of Defense: March 26, 2015

The thesis of R.A. Nadisanka Rupasinghe is approved.

Dean Amir Mirmiran
College of Engineering and Computing

Dean Lakshmi N. Reddi
University Graduate School

Florida International University, 2015

ACKNOWLEDGMENTS

I would like to thank Dr. Walid Saad, Dr. Nazih Pala, and Dr. Hai Deng in my committee for their kind guidance and feedback which always motivated me in achieving the final goal of this research. Specially my major Professor Dr. İsmail Güvenç who guided me throughout this process and encouraged me all the time.

Further, I would like to specially thank Dr. Fujio Watanabe from DOCOMO Innovations, Inc., for fruitful discussions and useful feedback provided throughout the research.

Finally, I would like to thank my family for supporting me in many ways to complete my research work during this entire time duration.

ABSTRACT OF THESIS

WiFi AND LTE COEXISTENCE IN THE UNLICENSED SPECTRUM

by

R.A. Nadisanka Rupasinghe

Florida International University, 2015

Miami, Florida

Professor İsmail Güvenç, Major Professor

Today, smart-phones have revolutionized wireless communication industry towards an era of mobile data. To cater for the ever increasing data traffic demand, it is of utmost importance to have more spectrum resources whereby sharing under-utilized spectrum bands is an effective solution. In particular, the 4G broadband Long Term Evolution (LTE) technology and its foreseen 5G successor will benefit immensely if their operation can be extended to the under-utilized unlicensed spectrum.

In this thesis, first we analyze WiFi 802.11n and LTE coexistence performance in the unlicensed spectrum considering multi-layer cell layouts through system level simulations. We consider a time division duplexing (TDD)-LTE system with an FTP traffic model for performance evaluation. Simulation results show that WiFi performance is more vulnerable to LTE interference, while LTE performance is degraded only slightly.

Based on the initial findings, we propose a Q-Learning based dynamic duty cycle selection technique for configuring LTE transmission gaps, so that a satisfactory throughput is maintained both for LTE and WiFi systems. Simulation results show that the proposed approach can enhance the overall capacity performance by 19% and WiFi capacity performance by 77%, hence enabling effective coexistence of LTE and WiFi systems in the unlicensed band.

TABLE OF CONTENTS

LIST OF FIGURES

CHAPTER I

Introduction

With the emergence of new wireless applications and devices, the demand for radio spectrum has been dramatically increasing over the last decade. Cisco has recently predicted an 11-fold increase in global mobile data traffic between 2013 and 2018 [4], while Qualcomm has predicted an astounding 1000x increase in mobile data traffic in near future [5]. President Obama, in his memorandum [6], had foreseen this and specifically asked to make available a total of 500 MHz of spectrum over the next 10 years to support new applications and technologies. Further, National science foundation, with the launch of its *enhancing access to the radio spectrum (EARS)* solicitation, took the initiatives in exploring the opportunities for a more effective utilization of the radio spectrum [7].

Effectively sharing the under-utilized spectrum bands by different wireless technologies can bring enormous opportunities in enhancing radio spectrum access. Specially, the 4G broadband Long Term Evolution (LTE) technology and its foreseen 5G successor, which will be the dominant technologies to keep up with the emerging traffic demand, can benefit immensely from spectrum sharing as they can get access to more spectrum resources. Identifying this potential, the 3GPP standardization group has recently initiated a study item (SI) on licensed-assisted access (LAA) using LTE in the unlicensed spectrum [8]. Through LAA, LTE operation is expanded to the unlicensed band, where it can coexist with the other deployments such as the WiFi technology. LTE can achieve carrier aggregation utilizing licensed spectrum for primary carrier and the unlicensed spectrum for secondary carrier.

In order to access unlicensed spectrum by LTE, properly designed coexistence techniques are essential. As proposed in SI [8], LAA operation of LTE should not impact WiFi services more than an additional WiFi network on the same carrier. Hence, it is of utmost importance to develop resilient coexistence mechanisms for the simultaneous operation of WiFi and LTE in the unlicensed spectrum. With that, there will be significant potential to enable broadband wireless communication with high data rates, that use LTE in the unlicensed spectrum.

In this research, first we evaluate the WiFi 802.11n and time division duplex (TDD)-LTE coexistence performance in the 5 GHz industrial, scientific and medical (ISM) band considering a multi layer cell layout. A comprehensive system level simulator is developed by incorporating TDD-LTE and WiFi 802.11n, medium access control (MAC)/ physical (PHY) functionalities [1] and a non-full buffer data traffic model [3] using Matlab, for accurate performance evaluations. With this simulator, extensive computer simulations are carried out to obtain insights on the WiFi-LTE coexistence behavior under several different realistic implementation scenarios.

Based on the results of initial coexistence performance evaluation, we propose a novel reinforcement learning (RL) based WiFi and LTE coexistence mechanism in the unlicensed spectrum. In particular, we use Q-Learning to dynamically configure transmission gaps in LAA periodically, based on its learnings from the environment. First, we evaluate the system performance under different duty cycles of the transmission gaps. Then, the performance of Q-Learning based dynamic duty cycle selection technique is evaluated. The simulation results show that the Q-Learning based approach improves overall system capacity performance by 19% and WiFi capacity performance by 77% compared to the scenario with fixed duty cycles that yields the highest aggregate capacity.

The rest of the thesis is organized as follows. In Chapter II, we provide a summary of different techniques proposed in the literature for facilitating the coexistence of different

wireless technologies. Chapter III presents initial WiFi-LTE coexistence performance evaluation results while providing details about simulator implementation and different scenarios considered. The novel Q-Learning based dynamic duty cycle based approach for LTE transmission to facilitate simultaneous operation of WiFi-LTE in the unlicensed spectrum is explained in detail in Chapter IV. Finally, Chapter V provides concluding remarks.

CHAPTER II

Literature Review

This section summarizes coexistence studies / techniques proposed in the literature between different wireless technologies. These studies mainly focus on the simultaneous operation of IEEE 802.15.4 and WiFi, LTE and Wide band - code division multiple access (W-CDMA), and WiFi and LTE in TV white space, ISM bands and also licensed spectrum.

2.1 Coexistence Between Different Wireless Technologies

Simultaneous operation between different wireless technologies in the same frequency band is studied in the literature. Coexistence impact of IEEE 802.11 b/g on the IEEE 802.15.4 is studied in [9]. In that, a coexistence model between IEEE 802.15.4 and IEEE 802.11 b/g is presented. Based on the transmit power and receiver sensitivity between two technologies, three coexistence regions have been identified in the model. In [10], coexistence performance of IEEE 802.15.4 with Bluetooth and WiFi is evaluated based on differences in the implementation aspects of these technologies. To facilitate the coexistence between IEEE 802.11 and Bluetooth, an adaptive frequency hopping mechanism to modify Bluetooth frequency hopping sequence and an interference aware scheduling strategy for Bluetooth, are proposed in [11].

An experimental study of coexistence issues between IEEE 802.15.4 and IEEE 802.11b is presented in [12]. In that, insights on the coexistence performance between these technologies is studied focusing on physical layer and as well as network/transport layers aspects. Authors suggest that this study helps in taking efficient actions to the problems arise

due to the coexistence of IEEE 802.15.4 and IEEE 802.11b. Another measurement based coexistence study between IEEE 802.11 and IEEE 802.15.4 is presented in [13]. In that, observed results show that IEEE 802.11 performance degrades considerably with this coexistence. On the other hand, [14] proposes an interference mediation scheme as a solution to performance degradation experienced by IEEE 802.15.4 due to the coexistence with IEEE 802.11b in the ISM band. Interference mediation is achieved through an interference mediator which coordinates between two technologies. In [15], laboratory experiments are carried out to identify ZigBee communication performance in all 16 Zigbee transmission channels, under WiFi interference. Performance is evaluated by varying transmit power, communication channels and communication distance in ZegBee transmission.

Mechanisms to operate ultra-wideband (UWB) and WiMAX devices in the same frequency band are studied in [16], using spectrum sensing techniques. In that, detect-and-avoid mechanisms are proposed for mitigating interference. In [17], WiFi and WiMaX coexistence in adjacent frequency bands is analyzed; to overcome adjacent channel interference, time sharing techniques are proposed across different technologies.

2.2 Coexistence Between LTE and Other Wireless Technologies

To facilitate simultaneous operation of LTE with other wireless technologies in the same frequency band, there are several studies/techniques proposed in the literature. In [18], an approach to facilitate the coexistence between multicarrier and narrow band (i.e., LTE and W-CDMA) technologies in the same frequency band, is presented. In that, by treating both co-channel signals as desired signals, they are enhanced in an iterative manner. In every iteration, one co-channel signal is subtracted from the received signal successively in order to obtain a better estimate of the other co-channel signal. A receiver which suppresses the co-channel dominant interference by blanking frequency-domain samples where the desired and interfering signals ovarlap, is proposed in [19], to facilitate simultaneous op-

eration of different wireless technologies in the same band. A coexistence study about downlink high-speed railway communication system with TDD-LTE is presented in [20]. In that, it has been identified that when these two technologies are deployed in the same frequency band, the high speed railway communication system is severely affected from interference. Additional isolation schemes are proposed as a solution to over come this problem. In [21], coexistence study between LTE and digital video broadcasting 2^{nd} generation terrestrial (DVB-T2-Lite) system, is presented. The paper basically analyzes impact of LTE on DVB-T2-Lite system, when they operate in the same frequency band. In another coexistence study, coexistence performance is evaluated between LTE and mobile satellite services (MSS) systems [22]. Based on the simulation results it has been concluded that, for LTE DL, there is not much of an issue from the coexistence whereas for LTE uplink (UL), severe performance degradation is observed due to interference.

2.3 Coexistence Between WiFi and LTE

Simultaneous operation of LTE and WiFi in the same frequency band is receiving high attention recently as this can be an effective solution for the spectrum shortage problem. This potential has also been identified by the 3GPP standardization group and they recently initiated a SI for LAA operation of LTE which is expected to be completed by June 2015. This SI will be followed by a LTE Rel-13 work item (WI).

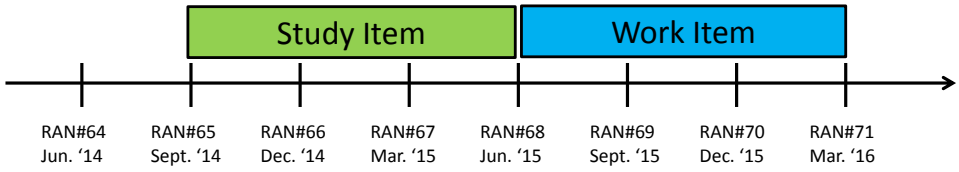

Figure 1: LAA standardization time line [2].

There are several objectives identified in this SI for proper LAA operation of LTE in the unlicensed spectrum. Among them, defining an evaluation methodology and possible

scenarios for LTE deployments in the unlicensed spectrum, identifying and defining design targets for coexistence with other unlicensed spectrum deployments, identifying and evaluating physical layer options and enhancements for LTE to meet the requirements and targets for the unlicensed spectrum deployments, and identifying the need of enhancements to LTE radio access network (RAN) protocols to support deployment in the unlicensed spectrum, are important. When coexisting with WiFi, it has been specifically mentioned in the SI that LAA should not impact WiFi services more than an additional Wi-Fi network on the same carrier. Further, when identifying and defining design targets, facilitating coexistence between different LAA operators is also considered as an important objective in the SI. For LAA operation of LTE, main focus will be on 5 GHz unlicensed spectrum. It is suggested to reuse most of the current features of LTE, when extending LTE operation to the unlicensed spectrum [8].

Possible operating modes and deployment scenarios for LAA operation of LTE are proposed in [23]. Regarding possible operating modes, the unlicensed spectrum can be used for carrier aggregation (CA) only for downlink (DL) and for both UL and DL, as can be seen from Fig. 2. Here the primary carrier is from the licensed spectrum whereas the secondary carrier is from the unlicensed spectrum. Initially it is expected to give high priority for CA based DL only LAA deployment. After that, for both UL and DL, CA from the unlicensed band will be introduced. [8].

Different possible deployment scenarios for LAA are discussed in [23, 24]. Due to regulatory conditions, transmit power is limited in most of the unlicensed bands. Further, as unlicensed spectrum is usually from higher frequency bands compared to the licensed spectrum, achievable coverage with unlicensed bands is comparatively low. Hence as shown in Fig. 3 (a), by deploying both the licensed and the unlicensed carriers together and utilizing licensed carriers for control data transmission, better performance can be achieved.

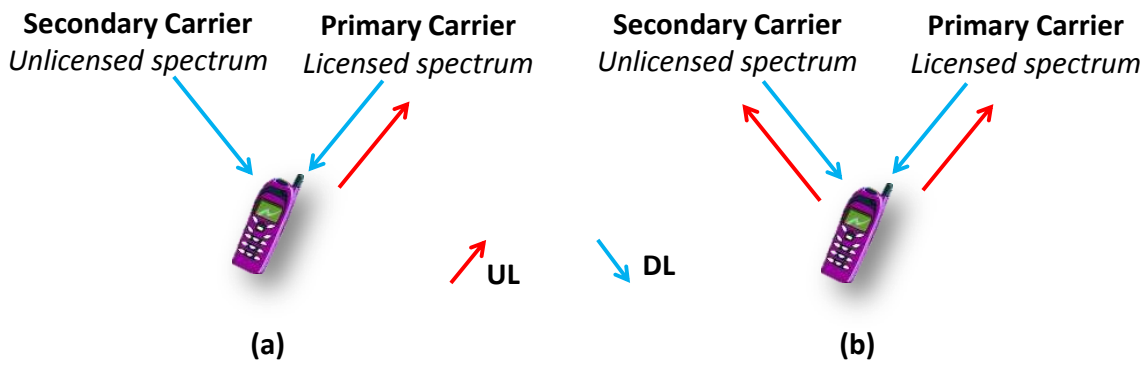

Figure 2: LTE uses secondary carrier from the unlicensed spectrum: *(a)* only for DL carrier aggregation. *(b)* Both for UL and DL carrier aggregation.

Non-Co-located deployment (see Fig. 3 (b)) is another possibility where macro LTE base stations (BSs) use the licensed spectrum while small cell LAA BSs utilize the unlicensed spectrum. Inter-site aggregation between macro and LAA BSs is achieved through a high speed backhaul [23].

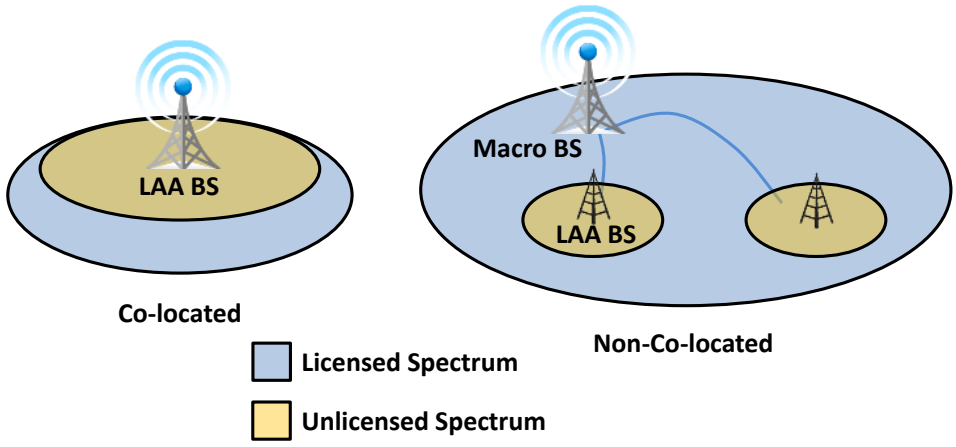

Figure 3: LAA BSs operating in the unlicensed spectrum.

Possible sub-bands within 5 GHz unlicensed spectrum is investigated in [25] for LAA operation. It is suggested that 5724 MHz - 5825 MHz is a good candidate for most regions of the world for LAA operation as it allows highest possible transmit power compared to other sub-bands. As can be seen from Fig. 4, within some sub-bands dynamic frequency

selection (DFS) and transmit power control (TPC) are necessary for the operation. In addition, 5350 MHz - 5470 MHz and 5850 MHz - 5925 MHz are also in favor of LAA operation with revised or new regulations.

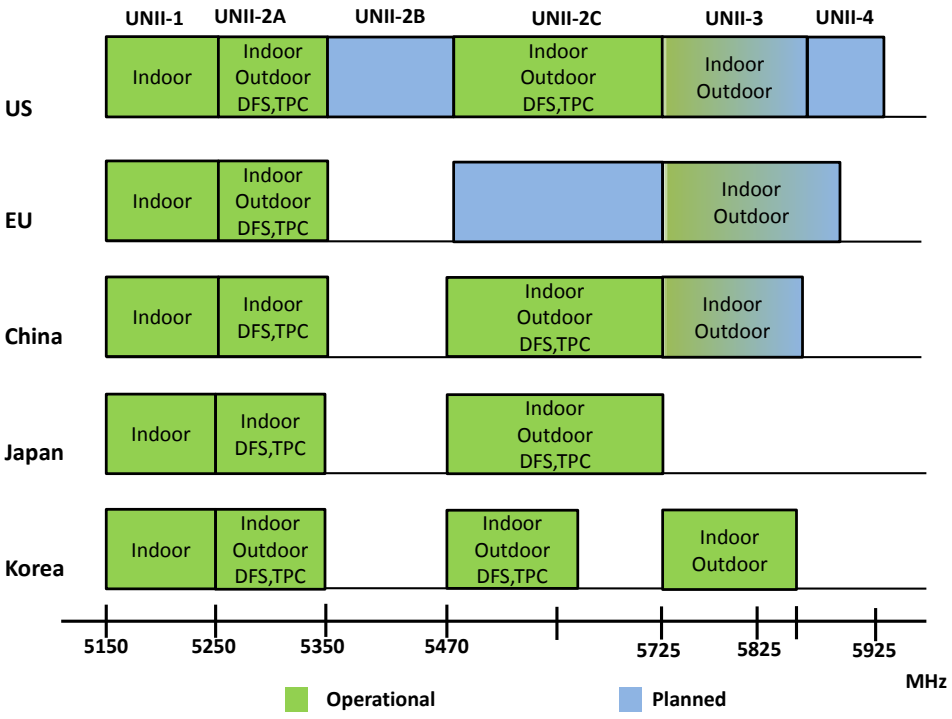

Figure 4: Available Sub-bands in 5 GHz unlicensed spectrum [25]. *Transmit power control* (TPC) and *Dynamic frequency selection* (DFS) are necessary for transmission in some of the sub-bands.

However, there are some more regulatory conditions defined for some regions in the world when operating in 5 GHz unlicensed band. Eliminate/mitigate interference to radar transmissions is one such requirement applicable to most of the regions in the world. For Japan, 4 ms maximum transmission duration and Listen-Before-Talk (LBT) transmission have to be satisfied for operating in the unlicensed spectrum. LBT, maximum transmission duration limit and transmission bandwidth are important regulatory conditions for the unlicensed band operation in Europe [26]. In [25], a case study about feasibility of introducing DFS for LAA mainly to avoid LAA getting interfered to radar transmission is presented.

Some interesting motivating factors for deploying LAA in the unlicensed spectrum are presented in [27]. Among them, achievable capacity enhancement, seamless connectivity, better handing of operation and maintenance (O&M) and quality of service (QoS) issues, utilizing same core network with the licensed band LTE, and longer range and higher efficiency than WiFi, are important.

Before initiating the SI in Sep. 2014, 3GPP group organized a workshop in Jun. 2014, fully focusing on LAA operation of LTE in the unlicensed spectrum [28]. In that, some interesting solutions/studies were presented by different companies [24, 27, 29–38]. In [29] from [28], experiment based and simulation based studies of WiFi and LAA coexistence are carried out to get insight on the coexistence performance. Based on the experimental study, it is concluded that, for single WiFi access point (AP) and LAA BS scenario, LAA outperforms WiFi in terms of both coverage and cell throughput. Further, from the simulation based study it has been shown that, with carrier selection based LAA transmission, WiFi-LAA coexistence performance can be enhanced. In [39], coexistence between WiFi and LTE (900 MHz) is investigated considering single floor and multi floor indoor office scenarios. By using system level simulations, it has been shown that the WiFi performance affected heavily when WiFi and LTE operates simultaneously in the unlicensed spectrum.

In [27] also some interesting simulation results from a LAA-WiFi coexistence study are presented. In that, it is shown that the achievable aggregate throughput when two LAA networks (operators) operate in fully overlapping channels is larger compared to two WiFi networks operating in the same manner. Further, by deploying LBT based LAA transmission with a fairness algorithm and WiFi in a fully overlapping unlicensed band, it is shown that higher aggregate throughput can be obtained compared to two WiFi networks operating in the same channel.

Qualcomm in [40–42] provides some important studies about facilitating WiFi-LAA coexistence in the unlicensed spectrum. As main advantages of LTE operation in the unlicensed spectrum better coverage and increased capacity are identified. Since LTE is a coordinated and managed architecture, LTE in the unlicensed spectrum can offer higher performance than WiFi for the same transmit power. Based on their initial studies, it has been shown that it is possible to achieve two fold or higher performance with LAA as compared to WiFi. For an instance, LTE operating in the unlicensed spectrum can provide twice the capacity of WiFi with the same number of nodes.

In order to achieve harmonious coexistence where LTE-Advance (LTE-A) can become a good neighbor to WiFi, [41] proposes some interesting solutions. In that, LAA small cells carry out initial channel search to identify suitable channels in 5 GHz band with minimum observed interference level. Based on the interference level, they dynamically adjust the channel for continued interference avoidance. However if there is no clear channel available, *carrier sensing adaptive transmission* (CSAT) mechanism is proposed where duty cycle based LTE-A transmission is deployed. This solution is specially applicable to countries where there is no regulatory requirement for LBT waveform for the unlicensed band (i.e. US, China and South Korea). CSAT mechanism can ensure fair spectrum sharing with WiFi nodes even in a very dense LTE-A nodes deployment. Medium sensing duration is longer in CSAT compared to regular LBT mechanisms. Based on the sensed medium activities of other technologies, the duty cycle of transmission vs gating off will be defined by CSAT [42]. Further, it is proposed that the unlicensed spectrum access by LTE-A small cells should be done *on-demand* basis, meaning that only the small cells having active users are able to transmit in the unlicensed spectrum. This type of an approach is possible since there is a mandatory anchor from the licensed band. Transmit power adjustment is also proposed for minimizing the interference to WiFi.

Coexistence performance of LAA and WiFi based on different deployment scenarios is evaluated in [43] with LBT implemented on LAA. Based on the simulation result it has been shown that the coexistence performance is very sensitive to deployment. For an example, in dense deployments, WiFi median throughput performance degrades when coexisting with LAA. But in sparse deployments there is not much difference in WiFi median throughput performance when coexisting with LAA. Further, based on the indoor/outdoor mixed deployment evaluations, it has been identified that LAA requires *request-to-send* (RTS) and *clear-to-send* (CTS) like operation to achieve fairness and spectral efficiency, due to hidden node problem. Another interesting observation in this evaluation is that, LBT based LAA operation shows better balancing between improving fairness and maximizing overall spectral efficiency compared to 50% duty cycle based transmission.

In [44], for the simultaneous operation of WiFi and LTE in the TV white space, two techniques are proposed to facilitate interference management: 1) spectrum sensing (LBT) by LTE, and 2) coexistence gap during which LTE refrain from transmitting. Frequency division duplexing (FDD)-LTE is considered here and LTE BS attempts to access the channel only at pre-assigned time instants denoted as *transmission opportunities* which are aligned with sub-frame boundaries. With LBT approach for DL transmission, LTE BS performs energy detection based sensing of the medium for predefined time interval (during *transmission opportunity*). If the channel is sensed to be idle (detected energy is below a threshold), LTE BS accesses the channel and starts DL transmission. This transmission will take place for fixed number of sub frames and there will not be any sensing involved within this duration. The DL transmission is followed by a *coexistence gap*, to enable other secondary users such as WiFi to access the channel.

To access license-exempt band for CA, LBT based LTE transmission along with RTS/CTS message exchange prior to starting the actual LTE transmission is proposed in [45]. LTE BS will sense the license-exempt band before transmitting and if the medium is detected to

be idle, LTE BS will start transmission. For UL, UE is responsible for sensing the medium before initiating a UL transmission. However, unlike in WiFi, the proposed LBT approach for LTE does not consider a random backoff and once the medium is detected to be idle, LTE BS/UE will start the transmission. LBT based approach proposed in [33] for LTE transmission considers handling of both inter-radio access technology (RAT) interference and intra-RAT interference. To handle inter-RAT interference, energy detection based LBT approach is proposed, whereas to handle intra-RAT interference, LBT based on cross correlation detection is proposed.

Blank sub frame allocation technique by LTE is introduced in [46] to facilitate simultaneous WiFi and LTE operation in the unlicensed spectrum. During silent subframes referred to as blank subframes, LTE refrains from transmitting and as a result WiFi gets more opportunities to access the channel. This mechanism is very much similar to almost-blank-subframe (ABS) concept introduced in LTE - Rel.10 for enhanced inter-cell interference coordination (eICIC). However, unlike in ABS, subframe blanking mechanism introduced here will not transmit any reference signals (RSs) during blank subframe. Similar approach is considered in [47], in which LTE allocates silent gaps with a predefined duty cycle to facilitate better coexistence with WiFi. However, this technique will refrain from achieving maximum gain of LTE operation in the unlicensed spectrum due to its discontinuous transmission. An UL power control based mechanism is evaluated for LTE systems in [48] to allow simultaneous operation of WiFi and LTE in the unlicensed spectrum. In that, LTE UL transmit power is reduced in a controlled manner based on interference measurements, generating more transmission opportunities to WiFi. Exchanging spectrum allocation information between WiFi and LTE via a common database is considered in [34] for enabling simultaneous access to the unlicensed spectrum by LTE and WiFi.

In [23], performance degradation due to multiple operators utilizing the same unlicensed band, is studied. Simulations are carried out for a 2 operator case and it is shown

that the user experience degrades heavily due to uncoordinated LAA BSs deployments. As viable solutions [23] suggests: 1) an agreement could be reached between multiple operators for orthogonal/exclusive use of the unlicensed spectrum within a given region. This can totally avoid inter-operator interference, with the cost of potentially inefficient use of spectrum due to the lack of dynamic spectrum sharing, and 2) introduce some dynamic schemes where unlicensed spectrum can be shared between operators. In this case, operators can occupy/release the unlicensed spectrum through some dynamic coordination and information exchange between them. To achieve coordination between different operators, [23] suggests that the monitoring of LTE transmission over the air interface could provide potentially enough cooperation information between LTE transmissions of different operators. A game theoretic approach to share unlicensed spectrum between several operators is proposed in [49]. In that, it is shown that, selfish and strategic operators find that being entirely non-cooperative is a Nash equilibrium; yet cooperative sharing is to the best interest of all. Further some mechanisms have been designed such that operators seek a subgame perfect Nash equilibrium where all operators are fully cooperative.

In [50], user equipment (UE) side necessary enhancements for the LTE unlicensed band operation is discussed. For the DL only CA from the unlicensed spectrum, channel quality information (CQI) has to be sent by the UE for the unlicensed band as well. Further, when the unlicensed band transmission introduces to both UL and DL CA, radar detection and LBT has to be implemented on UE side.

In this thesis, we propose a RL based coexistence mechanism to facilitate simultaneous operation of WiFi and LTE in the unlicensed spectrum. Through system level simulations, first, initial coexistence performance evaluation is carried out [51]. After that, proposed Q-Learning based coexistence mechanism is implemented and performance is evaluated [52]. Next few sections will provide detailed description about initial performance evaluation and proposed Q-Learning based WiFi and LAA coexistence mechanism.

CHAPTER III

WiFi-LTE Coexistence Performance Evaluation

In order to develop effective coexistence techniques, it is of utmost importance to study the coexistence performance between WiFi and LTE. From that, it is possible to identify which technology will be suffering heavily from this coexistence and what can be the possible solutions to facilitate this coexistence. Hence in this section, we evaluate WiFi-LTE coexistence performance under different criterias.

First, coexistence performance under different LTE traffic arrival rates is evaluated. Then, WiFi-LTE coexistence performance under different LTE TDD configurations with different duty cycles of UL subframes, is studied. Finally, coexistence performance with different path loss compensation factors is analyzed. The simulation results provide useful insights on PHY/MAC operating regimes, which will help in developing effective coexistence techniques for LAA.

3.1 Deployment Scenario

In order to evaluate the coexistence challenges and related interference management methods for LAA operation of LTE, we consider a scenario as shown in Fig. 5, where M LAA BSs and WiFi APs are operating simultaneously in the unlicensed band. Each WiFi AP (LAA BS) consists of N WiFi stations (STAs) (LAA UEs), which are uniformly randomly distributed within the cell coverage area. TDD-LTE is considered and it is assumed that LAA BSs and LAA UEs are synchronized together all the time.

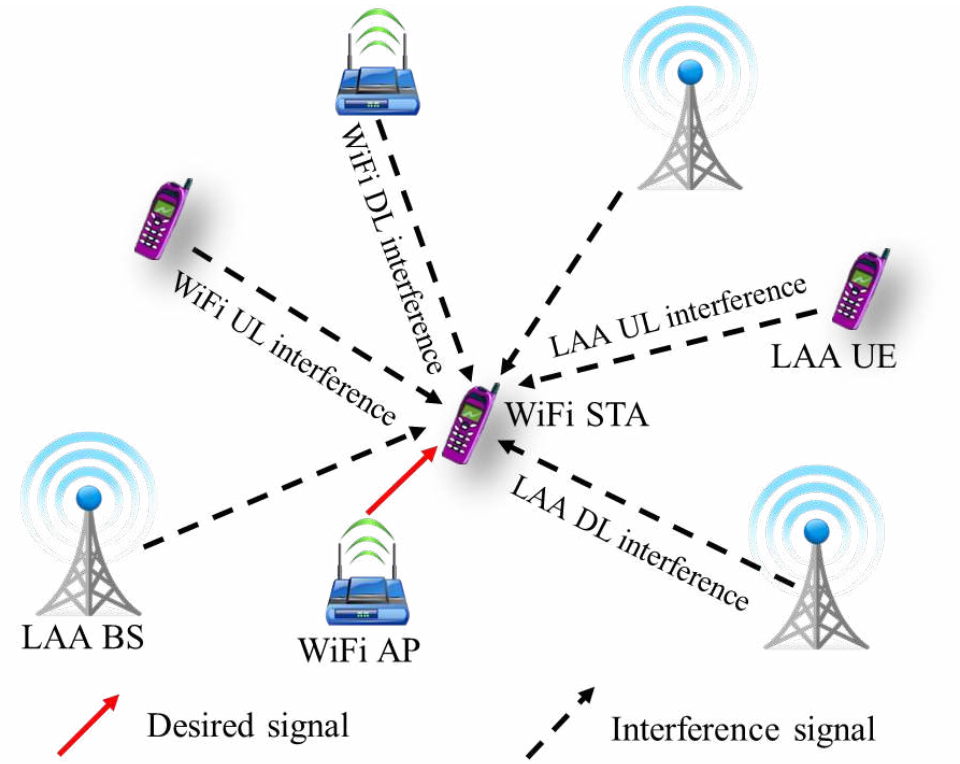

Figure 5: WiFi APs and LAA BSs operating simultaneously in unlicensed spectrum.

As shown in Fig. 5, due to simultaneous operation of WiFi and LAA in the unlicensed spectrum, targeted WiFi STA experiences interference from LAA DL/UL transmissions and other WiFi DL/UL transmissions. This will result in degrading the signal to interference plus noise ratio (SINR) at the targeted WiFi STA. In the same way, for WiFi UL transmissions and LAA DL/UL transmissions, WiFi and LAA simultaneous operation will increase interference and hence reduce SINR which will then degrade capacity performance. Due to *carrier sense multiple access with collision avoidance* (CSMA/CA) mechanism in WiFi [1], when coexisting with LTE, WiFi transmissions get delayed, further degrading WiFi capacity performance.

For both WiFi and LAA, we have considered a non full buffer traffic model as given in 3GPP FTP traffic model-2 [3]. In order to evaluate the capacity of WiFi and LAA for different simulation scenarios, a PHY layer abstraction is used. In particular, Shannon

capacity is calculated at the granularity of each WiFi OFDM symbol duration (4 μs) to obtain the number of successfully received bits. In all the simulations, wireless channel is modeled according to [3]. Both for WiFi and LAA, Indoor Hotspot (InH) scenario is considered when determining path loss and shadowing parameters used in the simulations.

For better understanding of coexistence mechanisms between the two technologies, brief summaries of PHY layer and medium access control (MAC) layer implementations of WiFi and LTE technologies are reviewed in the next sections.

3.2 Review of WiFi 802.11n MAC/PHY

In order to understand how LTE and WiFi systems can coexist with each other in the same frequency band, it is important to study the MAC implementation of both systems. In this section, MAC layer of WiFi will be reviewed, which is responsible for controlling the channel access procedure for multiple WiFi stations (STAs) to share the same wireless channel [1]. The MAC layer of WiFi is based on the carrier sense multiple access with collision avoidance (CSMA/CA) mechanism, where, if the wireless medium is sensed to be *idle*, an STA is permitted to transmit. However, if the channel is sensed to be *busy*, then the STA defers its transmission. The CSMA/CA mechanism particularly used in the IEEE 802.11 MAC is known as the *distributed coordination funtion* (DCF).

An example CSMA/CA scenario with four STAs (STA 1, STA 2, STA 3, and STA 4) which share the same wireless spectrum is shown in Fig. 6. STA 1 will start transmission of its *physical protocol data unit* (PPDU) and STA 2, STA 3 and STA 4 will back-off (will not access the medium) until STA 1 completes its transmission. Once the transmission of STA 1 is completed, PHY of the other three STAs start sensing the channel during a time period defined by the *arbitration inter frame space* (AIFS) parameter. At the end of the AIFS time period, STA 2, STA 3, and STA 4 will randomly back-off, and STA with the shortest back-off (STA 3) will occupy the medium for the next transmission. Subsequently,

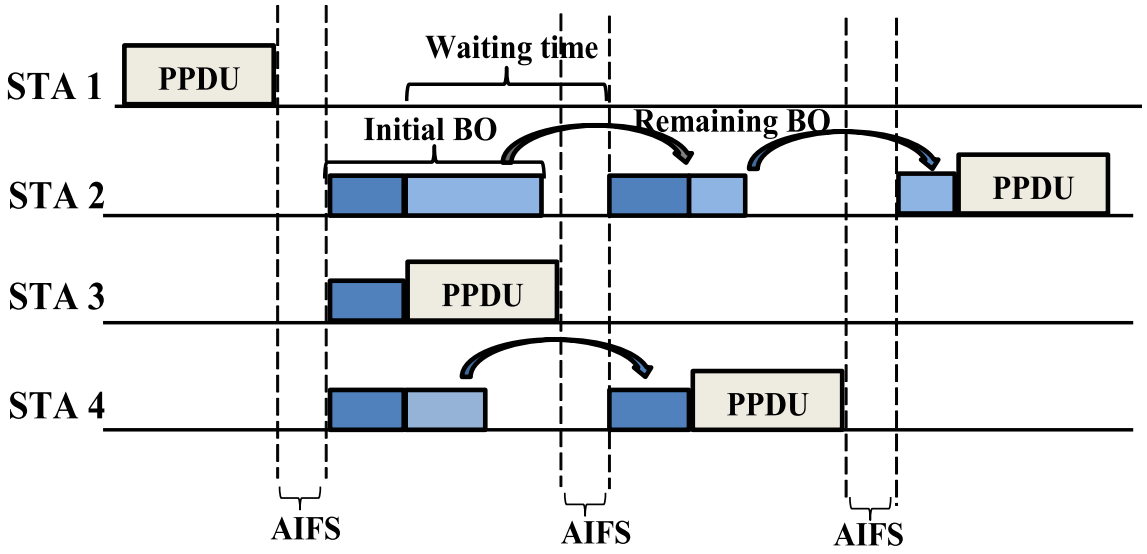

Figure 6: Back-off (BO) procedure in WiFi.

STA 2 and STA 4 will again go to back-off mode; however, as shown in Fig. 6, after the transmission of STA 3, STA 2 and STA 4 will use the remaining back-off time from the initial random back-off time. This will allow STAs to access the channel according to the order they start sensing the channel.

To gain a better insight about WiFi behavior during medium access, we describe the channel access procedure and physical carrier sensing mechanism known as *clear channel assessment* (CCA) of WiFi in the following subsections.

3.3 Enhanced Distributed Channel Access (EDCA)

The Enhanced distributed channel access (EDCA) is an extension of the basic DCF in WiFi which consists of four different types of access categories (ACs) (background, best effort, video, voice) to support prioritized quality of service (QoS) for different traffic types. As shown in Table 1, each category has different CSMA/CA parameters according to the traffic

Table 1: Default MAC parameters for different access categories of WiFi systems [1].

Access Category	AIFSN	CWmin	CWmax	TXOPlimit
Background	7	31	1023	0
Best effort	3	31	1023	0
Video	2	15	31	3.008 ms
Voice	2	7	15	1.504 ms
Legacy	2	15	1023	0

type. The AIFS time period of an AC can be determined as follows:

$$T_{\text{AIFS}}[\text{AC}] = T_{\text{SIFS}} + \text{AIFSN[AC]} \times T_{\text{slot}}, \tag{1}$$

where T_{SIFS} is the *Short inter frame space* time which is 16 μs, AIFSN[AC] is defined in Table 1 for each AC, and T_{slot} refers to the *slot time* which is 9 μs [1]. From (1), AIFS is the highest for *background traffic*, while it is the lowest for *video* and *voice* to ensure lower delay.

During the AIFS time period, if the medium is sensed to be *idle*, STAs will back-off for another random time period which is determined using the contention window (CW) parameters (CWmin, CWmax) shown in the Table 1. The random back-off time is a pseudo random integer drawn from a uniform distribution over the interval $[0, CW]$. The CW at an STA starts from the CWmin and effectively doubles on each unsuccessful *Aggregate MAC protocol data unit* (A-MPDU) transmission.

3.4 Clear Channel Assessment Based on Carrier Sense

The CCA is composed of two related functions: carrier sense (CS) and energy detection (ED). During CS by the PHY of a particular STA, if 1) the detected energy level is higher than the defined threshold (set to -82 dBm for WiFi), and 2) the header information of the PPDU currently occupying the channel is successfully decoded, that STA will back-off till the end of a PPDU transmission from a different STA. This is achieved through the *network*

allocation vector (NAV) which operates at the MAC layer. According to the information extracted from the header, the NAV will inform PHY that the channel will be busy till the completion of current PPDU transmission. As a result, PHY will start sensing again at the end of the current PPDU transmission.

3.5 Clear Channel Assessment Based on Energy Detection

While CCA based on CS detects the presence of a decodable WiFi signal, CCA based on energy detection (ED) allows an STA to detect the non WiFi energy level present on the current channel (e.g., an LTE signal). This can be due to another electromagnetic signal in the same frequency band, or due to unidentifiable WiFi transmission that may be corrupted and the header information of the PPDU can no longer be decoded. The ED threshold level is normally 20 dB higher than the corresponding WiFi energy level threshold [1]. If the medium is identified to be busy due to ED, the STA has to sense the medium every *slot time*, to determine whether the energy still exists. When WiFi and LTE operate in the same spectrum, WiFi access points (APs)/STAs have to follow this procedure more frequently before gaining the channel access. This will inversely affect the achievable throughput from WiFi (diminishing the performance on WiFi side), since the sensing time will increase when LTE interference is present.

3.6 WiFi PHY Abstraction

In order to evaluate the capacity of WiFi for different simulation scenarios, a PHY layer abstraction is used. In particular, Shannon capacity is calculated at the granularity of each WiFi OFDM symbol duration to obtain the number of successfully received bits.

Fig. 7 shows the WiFi PPDU format considered in simulations. *Physical service data unit* (PSDU) coming from MAC to PHY consists of one 64 kB A-MPDU. WiFi throughput is averaged over a one second time duration as shown in Fig. 8. During this simulation

Figure 7: WiFi PPDU format.

interval, there can be several PPDU transmissions and in between two transmissions there is a random wait time (T_{Rand}), which is determined using the FTP traffic model described earlier [3]. During that time period, it is assumed that there is no data in the WiFi AP/STA queue. Therefore, for throughput calculations, intervals where there are no packets in the queue are not taken into consideration.

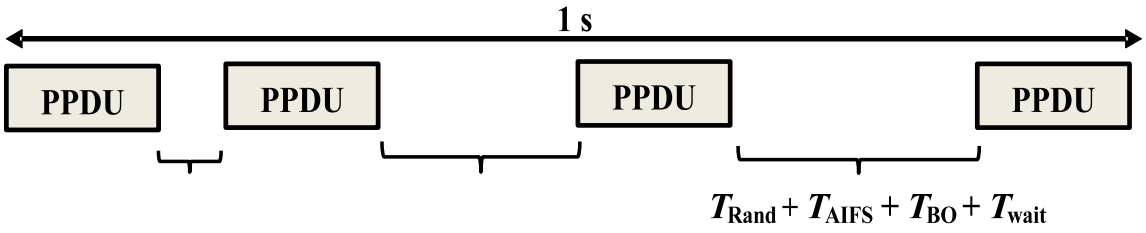

Figure 8: WiFi PPDU arrivals. WiFi capacity is averaged over 1 s time duration in the simulations.

Considering the aforementioned assumptions, number of successfully received bits, $N_{\text{B}}^{\text{WiFi}}$, for each transmitted WiFi OFDM symbol is given by:

$$N_{\text{B}}^{\text{WiFi}}(i) = B_{\text{WiFi}} \log_2 \left(1 + SINR_{\text{WiFi}}(i)\right) T_{\text{OFDM}}, \tag{2}$$

where B_{WiFi} is the allocated WiFi transmission bandwidth, $SINR_{\text{WiFi}}$ is the signal to interference plus noise ratio (SINR) of WiFi devices where interference term consists of both WiFi and LTE interference at the i^{th} OFDM symbol, and T_{OFDM} is the WiFi OFDM symbol duration.

Average WiFi capacity (C_{WiFi}) within one second duration as in Fig. 8 can then be written as

$$C_{\text{WiFi}} = \frac{\sum_{i=1}^{N} N_{\text{B}}^{\text{WiFi}}(i)}{N \times T_{\text{OFDM}} + \sum T_{\text{BO}} + \sum T_{\text{Wait}} + \sum T_{\text{AIFS}}}, \tag{3}$$

where N is the number of WiFi OFDM symbols transmitted during a one second duration, T_{AIFS} is the $AIFS$ time between two PPDU transmissions, and T_{BO} is the back-off time between two PPDU transmissions. Note that this back-off time will not capture the complete waiting time of a WiFi AP/STA which is expecting to access the channel. As described in Section 3.4, if the header information of currently ongoing WiFi transmission is successfully decoded, WiFi AP/STA can identify the time taken to complete that WiFi transmission. Therefore, as shown in Fig. 6, the total waiting time (T_{Wait}) between two PPDU transmissions should be captured separately for throughput calculations. In (3), $\sum T_{\text{BO}}$, $\sum T_{\text{Wait}}$ and $\sum T_{\text{AIFS}}$ capture total back-off, waiting and AIFS time within one second duration respectively.

3.7 Review of LTE MAC/PHY

Since the users are centrally scheduled by a base station, LTE MAC layer operation is quite different than the DCF based MAC approach in WiFi described in the previous section. In this thesis, TDD-LTE is considered for coexistence performance evaluation with different TDD configurations [53]. FTP traffic model-2 is implemented based on [3], where delay (d) between two packet arrivals is exponentially distributed with the probability density function given by

$$f(d) = \lambda \exp^{\lambda d}, \tag{4}$$

where λ is the packet arrival rate to the data queue. Fig. 9 shows how packets arrive at a user data queue based on the considered non-full buffer traffic model. Size of a data packet is fixed and assumed to be 0.5 MB.

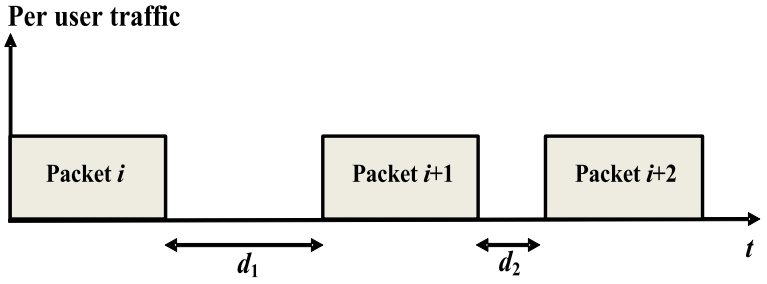

Figure 9: Traffic arrival to data queue according to FTP traffic model-2 [3]. The d_i is the delay between two data packet arrivals, which has an exponential distribution as outlined in (4).

The UL power control is achieved using the fractional power control mechanism in LTE as follows [53]

$$P_{\mathrm{UL}} = P_0 + \alpha PL + 10\log_{10} M, \tag{5}$$

where, P_{UL} is the UL transmitting power of the LTE UE, P_0 represents the base power level, PL is the path loss from LTE BS to LTE UE, and α is the path loss compensation factor. When $\alpha = 0$, no power control is applied in the uplink, and when $\alpha = 1$, path loss is fully compensated through power control. The number of RBs allocated to an LTE UE for UL transmission is denoted by M.

In all the simulations, wireless channel is modeled according to [3]. Both for WiFi and LAA, Indoor Hotspot (InH) scenario has been considered when determining path loss and shadowing parameters used in the simulations.

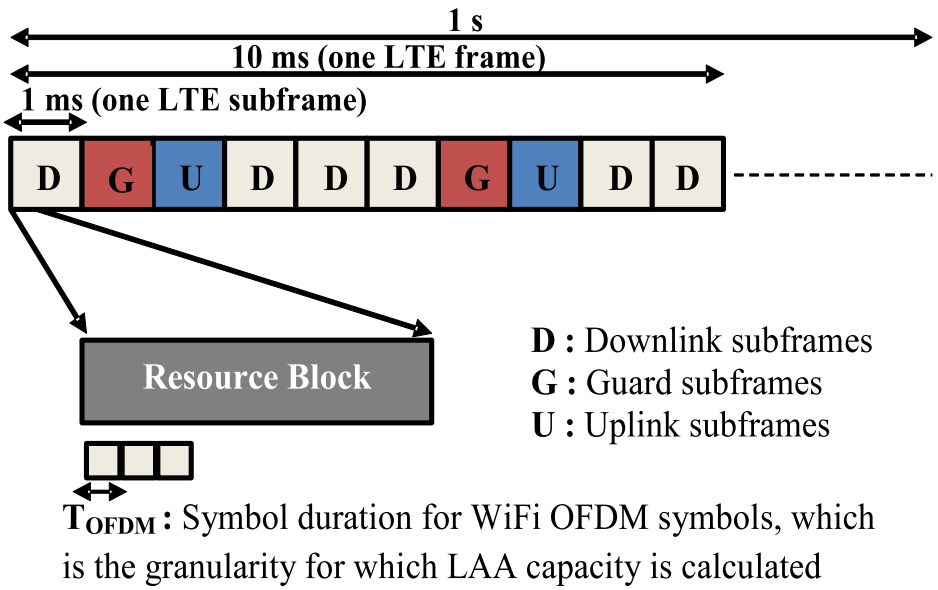

Figure 10: LAA capacity is captured over each WiFi symbol duration. It is then averaged over 1 s time duration in the simulations.

3.8 LTE PHY Abstraction

Similar to WiFi capacity abstraction, Shannon capacity equation has been used for LAA PHY abstraction. Due to WiFi OFDM symbol transmissions, interference at LAA changes with a time granularity of T_{OFDM}. Number of successfully received bits for LAA is then calculated for T_{OFDM} time granularity, and aggregated over one second duration (Fig. 10). As opposed to LAA, WiFi STAs do not use UL power control and all the time transmit at full power (23 dBm). Hence, observed interference at LAA BS and LAA UE due to WiFi UL / DL transmissions are similar. Number of bits received at LAA BS/UE during i^{th} T_{OFDM} time interval within one second is given by

$$N_{\text{B}}^{\text{LAA}}(i) = B_{\text{LAA}} \log_2 \left(1 + SINR_{\text{LAA}}(i)\right) T_{\text{OFDM}}, \tag{6}$$

where B_{LAA} is the allocated LAA bandwidth, $SINR_{\text{LAA}}$ term captures both WiFi and LAA interference at LAA BS/UE, and B_{LAA} directly relates to the number of RBs allocated dur-

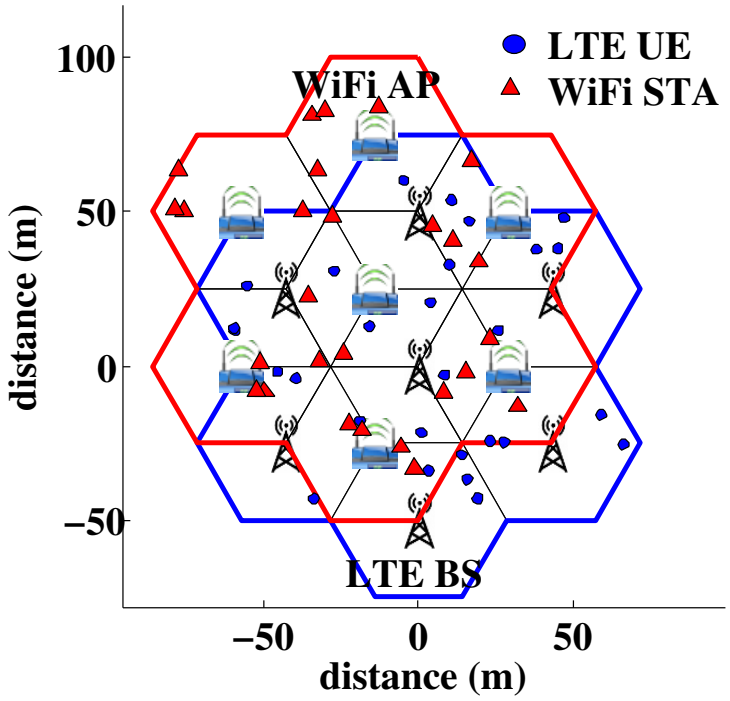

Figure 11: WiFi APs and LAA BSs in a multi layer cell layout.

ing a TTI. As the traffic is not full buffer, depending on the allocated RBs, WiFi interference at LAA is calculated.

LAA capacity in DL(UL) (C_{LAA}) is averaged over one second duration and can be calculated as

$$C_{\mathrm{LAA}} = \frac{\sum_{i=1}^{M} N_{\mathrm{B}}^{\mathrm{LAA}}(i)}{M \times T_{\mathrm{OFDM}}}, \tag{7}$$

where M represents number of T_{OFDM} time intervals within one second (Fig. 10) with LAA DL (UL) transmission exist.

Table 2: WiFi PHY/MAC parameters.

Parameter	**Value**
Transmission scheme	OFDM
Bandwidth	20 MHz
DL/UL Tx Power	23 dBm
AC	Best Effort
MAC protocol	EDCA
Slot time	9 μs
CCA-CS threshold	-82 dBm
CCA-ED threshold	-62 dBm
No. of service bits in PPDU	16 bits
No. of tail bits in PPDU	12 bits
CW size	$U(0,31)$
Noise figure	6 [1]
Traffic model	FTP Traffic model-2 [3]

3.9 Simulation Results Discussion - Initial Coexistence Performance Evaluation

Computer simulations are carried out to gain insights related to coexistence performance of WiFi and LAA in the unlicensed band under different simulation configurations. We consider a two layer cell layout, one each for WiFi and LAA, as shown in Fig. 11. Each layer consists of $M = 7$ cells. There are $N = 10$ WiFi STAs (LAA UEs) associated with each WiFi AP (LAA BS). WiFi STAs (LAA UEs) move within the cell with a speed of 3 km/h.

In the simulator, CCA based on CS and ED mechanisms are implemented as described in Section 3.4 and Section 3.5. During channel sensing, if two or more WiFi transmissions are observed by a particular STA with energy level greater than the CS energy level threshold, it is assumed that the header decoding is not possible. This situation is handled as an ED problem. All the traffic is assumed to be from *best effort* AC. Hence, *Transmit Opportunity* (TXOP) allocated is zero as per Table 1. Accordingly, during a channel access, only one PPDU transmission is allowed. Other parameters used for WiFi MAC/PHY implementation are summarized in Table 2.

Table 3: LTE PHY/MAC parameters.

Parameter	**Value**
Transmission Scheme	OFDM
Bandwidth	20 MHz
DL Tx power	23 dBm
UL Tx power	PL based TPC
Frame duration	10 ms
Scheduling	Round robin
P_0	-106 dBm
α	1
TTI	1 ms
Traffic model	FTP Traffic model-2 [3]

TDD-LTE is considered in simulations and it is assumed that LAA BSs and LAA UEs are synchronized together all the time. LAA UEs report the observed DL SINR value during a DL transmission to the LAA BS, which is then used by the LAA BS to determine the number of RBs to be allocated for the next DL transmission. Round robin user scheduling is considered in DL and only one user is scheduled during each transmission time interval (TTI). Based on the number of LAA UE requests for UL transmission during one subframe, bandwidth (BW) is equally divided between them. All the LTE MAC/PHY parameters used in the simulator are given in Table 3. In the remainder of this section, we study the simulation results obtained for different WiFi and LAA coexistence scenarios. In all these scenarios, we focus on the performance of center cell in both WiFi and LAA cell layouts.

3.9.1 Coexistence Under Different LAA Traffic Arrival Rates

In Figs. 12 - 15, WiFi and LAA coexistence performance is presented for different LTE traffic arrival rates, $\lambda = 1.5, 2.5$. In Fig. 12, WiFi and LAA DL capacity is compared. From that, it can be seen that WiFi performance degradation is high compared to LAA when they coexist in the same frequency band. Results in Fig. 13 show the cumulative density functions (CDF) of WiFi DL SINR for different LAA traffic arrival rates. From

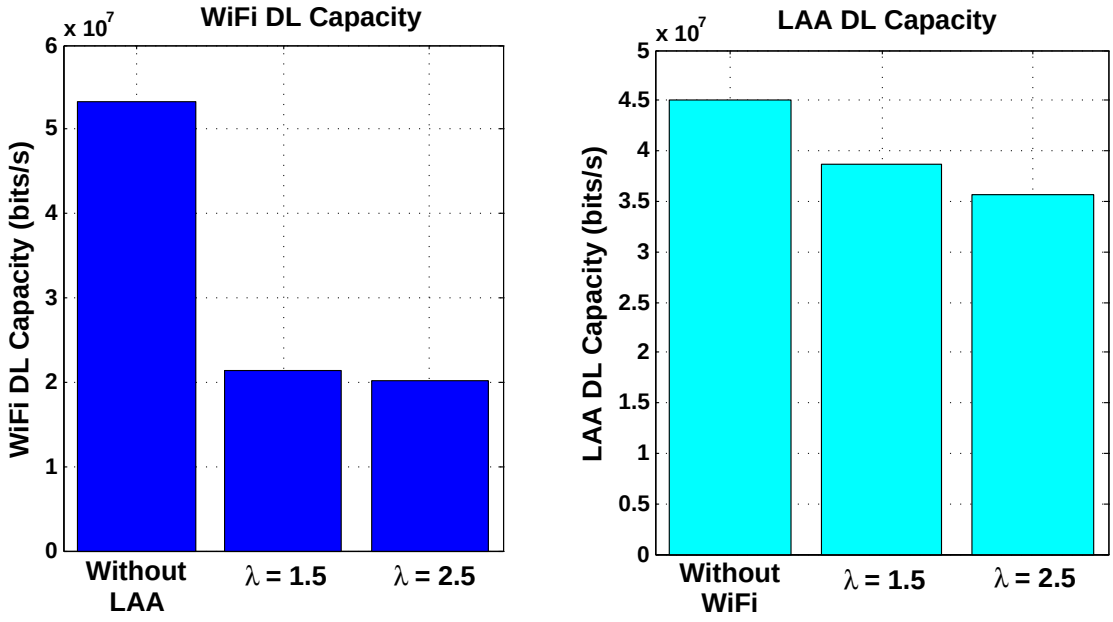

Figure 12: Average DL capacity (bits/s) of WiFi and LAA with different λ values.

these CDFs, it can be inferred that WiFi DL performance degradation is larger for higher λ.

Note that, in Fig. 13, there is a *step-like* behavior when LAA interference is present. This is because the LAA UL interference at the WiFi is lower when compared to the LAA DL interference, both of which can appear in a TD-LTE frame as shown in Fig. 10. This can be seen more clearly in Fig. 14, which plots the CDFs of LAA interference observed at WiFi devices. Over 30 dB difference in the interference power CDFs in Fig.14 manifests itself in the *step-like* behavior in the Fig. 13. As opposed to WiFi DL performance, results in Fig. 12 and Fig. 15 show that the LAA DL performance is not affected significantly from the presence of WiFi devices in the vicinity.

3.9.2 Coexistence Under Different LTE TDD Configurations

The TDD mode in LTE can be configured to have different number of DL and UL sub-frames, to support different traffic conditions. As shown in Fig. 16, in TDD configuration 1,

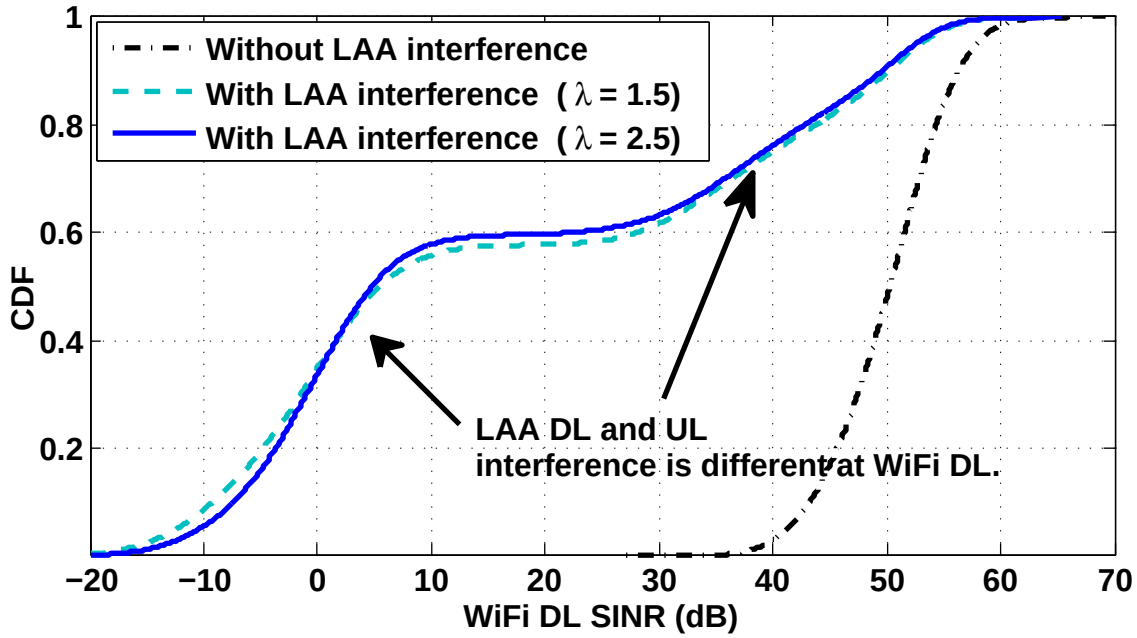

Figure 13: SINR distribution of WiFi DL with different LAA λ values.

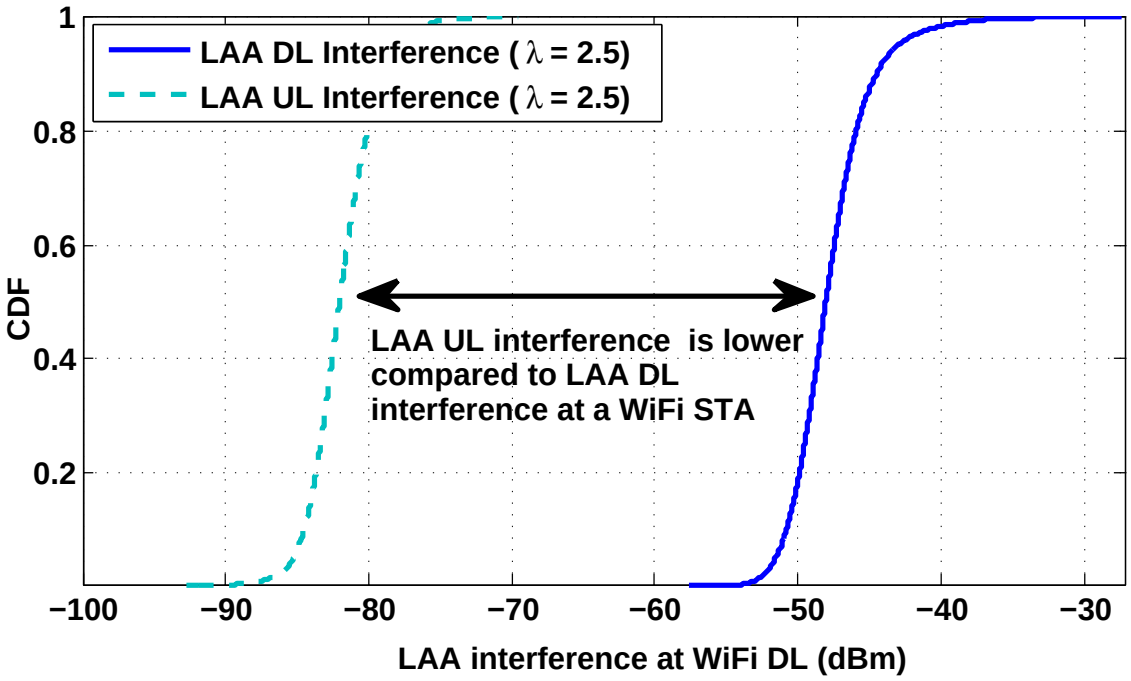

Figure 14: Interference distribution of LAA UL and DL at WiFi DL.

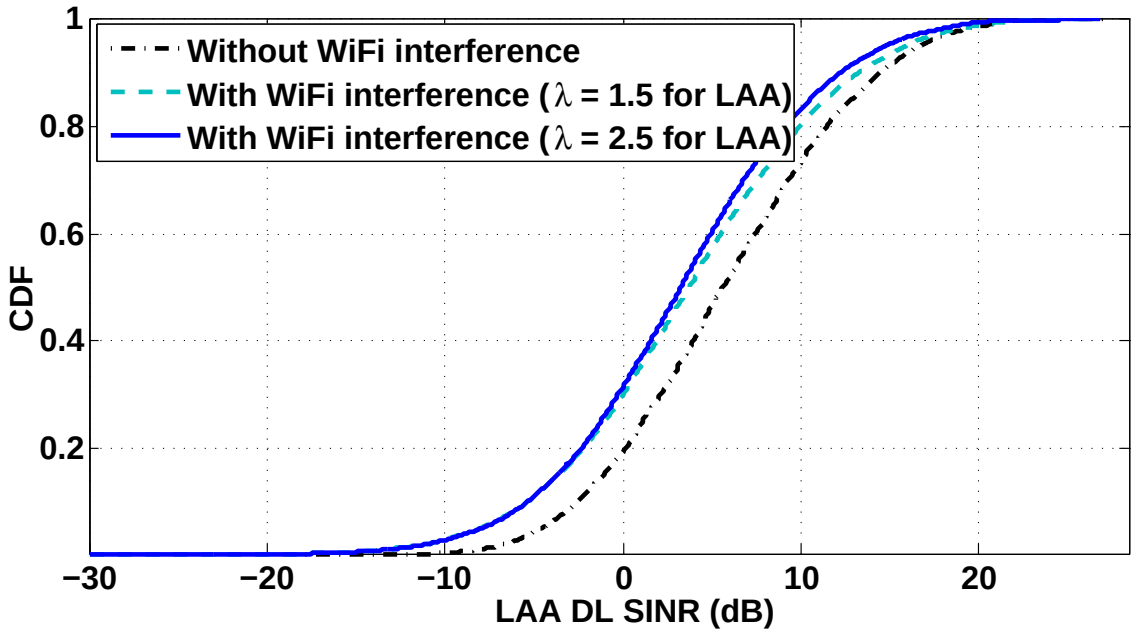

Figure 15: SINR distribution of LAA DL with different LAA λ values.

the number of UL subframes are two times that of configuration 2. The impact of different TDD configurations on the WiFi-LAA coexistence performance is shown in Figs. 18 - 19.

Fig. 18 compares WiFi and LAA DL capacity under different LTE TDD configurations. It can be seen that, with TDD configuration 1, WiFi capacity has increased. The main reason for that is in TDD configuration 1, number of UL subframes are larger when compared to TDD configuration 2. As explained in Section 3.9.1, LAA UL interference is lower compared to LAA DL interference. Hence, it can be inferred that LAA interference is lower with TDD configuration 1 when compared with configuration 2, and as a result, WiFi capacity increases with TDD configuration 1. On the other hand, LAA DL capacity under TDD configuration 1 is slightly reduced when compared to configuration 2. This is because, as WiFi gets more opportunities to transmit, interference from WiFi at LAA DL is higher with TDD configuration 1.

Fig. 17 plots the WiFi SINR CDFs with different LTE TDD configurations. As can be seen, WiFi SINR with TDD configuration 1 is improved when compared to TDD configu-

	Subframe Number									
	0	1	2	3	4	5	6	7	8	9
Config #1	D	G	U	U	D	D	G	U	U	D
Config #2	D	G	U	D	D	D	G	U	D	D

Figure 16: LTE-TDD configurations.

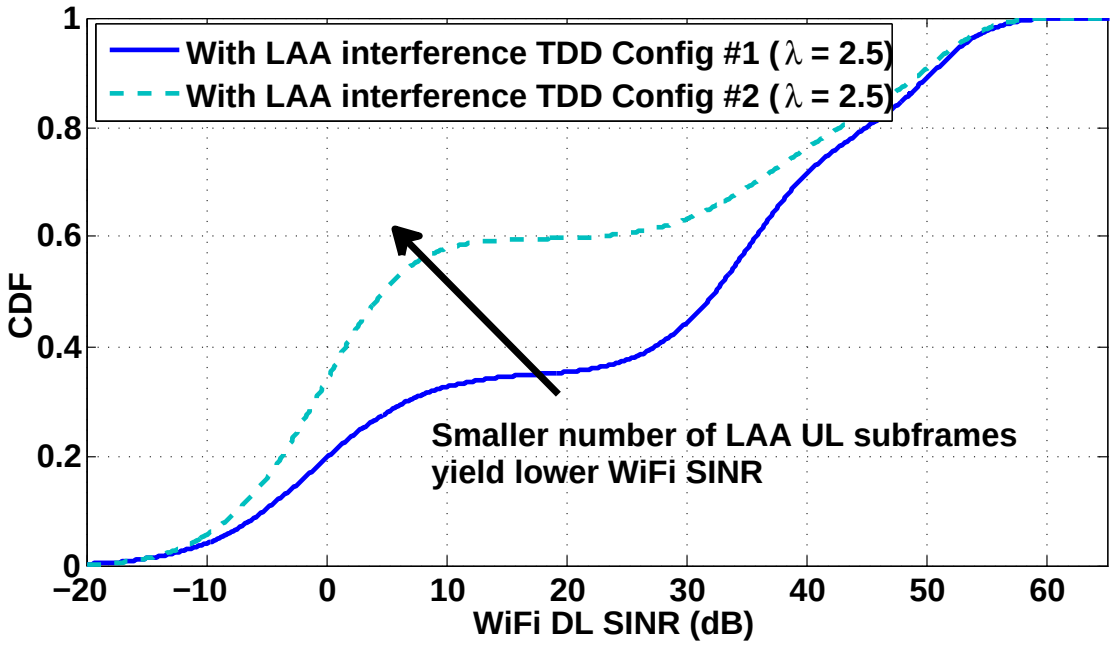

Figure 17: SINR distribution of WiFi DL with different LAA TDD configurations.

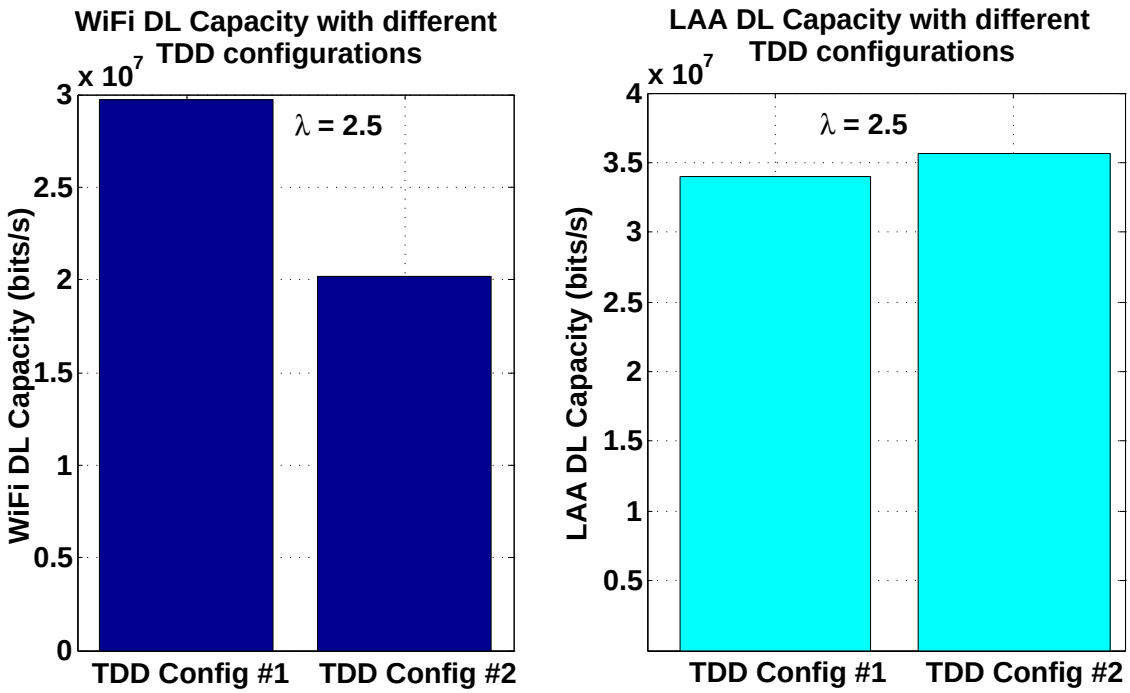

Figure 18: Average DL capacity (bits/s) of WiFi and LAA with different TDD configurations.

ration 2. This is because, as explained earlier, LAA interference at WiFi with TDD configuration 1 is lower compared to configuration 2. Therefore, when there are larger number of UL subframes, interference at WiFi is lower and as a result better WiFi performance can be observed.

Finally, Fig. 19 plots SINR CDFs of LAA DL for different TDD configurations. Slight SINR degradation in LAA DL can be observed for TDD configuration 1 when compared to configuration 2. As explained earlier, this is because of the increased WiFi interference with TDD configuration 1.

3.9.3 Impact of Path Loss Compensation Factors

To investigate the impact of fractional power (control based on (5)), the coexistence performance with different LTE α values is studied in Figs. 21 - 22. Fig. 21 shows LAA and WiFi DL capacities for different α values. It can be observed that the WiFi capacity is

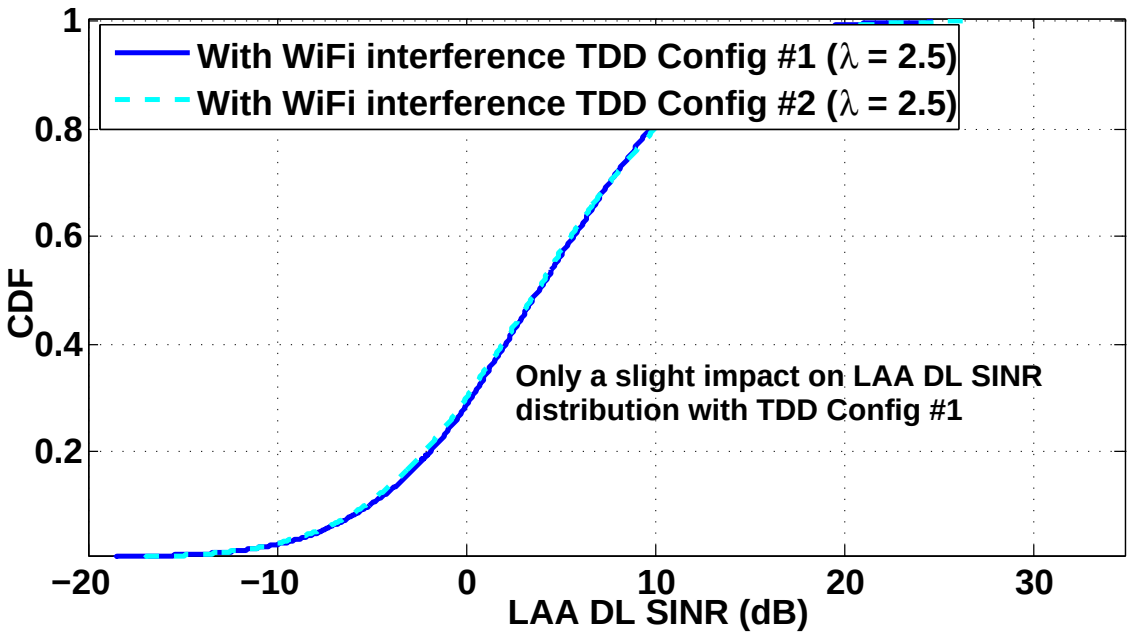

Figure 19: SINR distribution of LAA DL with different TDD configurations.

better with $\alpha = 0.5$, than with $\alpha = 1$. With smaller α values (<1), only a fraction of PL is compensated in LAA UL transmission. Hence, LAA interference at WiFi is lower with smaller α values due to low LAA UL transmission power, resulting in higher WiFi DL capacity. Fig. 20 plots WiFi DL SINR CDFs for different α values, which again shows the WiFi DL performance improvement with smaller α values due to lower LAA interference at WiFi.

Fig. 22 plots LAA UL/DL SINR CDFs with different α values. From that, it can be observed that LAA UL SINR with $\alpha = 0.5$ is around 35 dB lower when compared that with $\alpha = 1$. This is because, LAA UL transmit power is lower with $\alpha = 0.5$ compared to $\alpha = 1$ (according to (5)). However, as can be seen from Fig. 22, LAA DL SINR is not much affected from different α values and as a result, in Fig. 21, LAA DL capacity degradation is lower.

In this section, we studied WiFi and LAA coexistence performance under three different scenarios, considering a multi layer cell layout. Simulation results show that performance

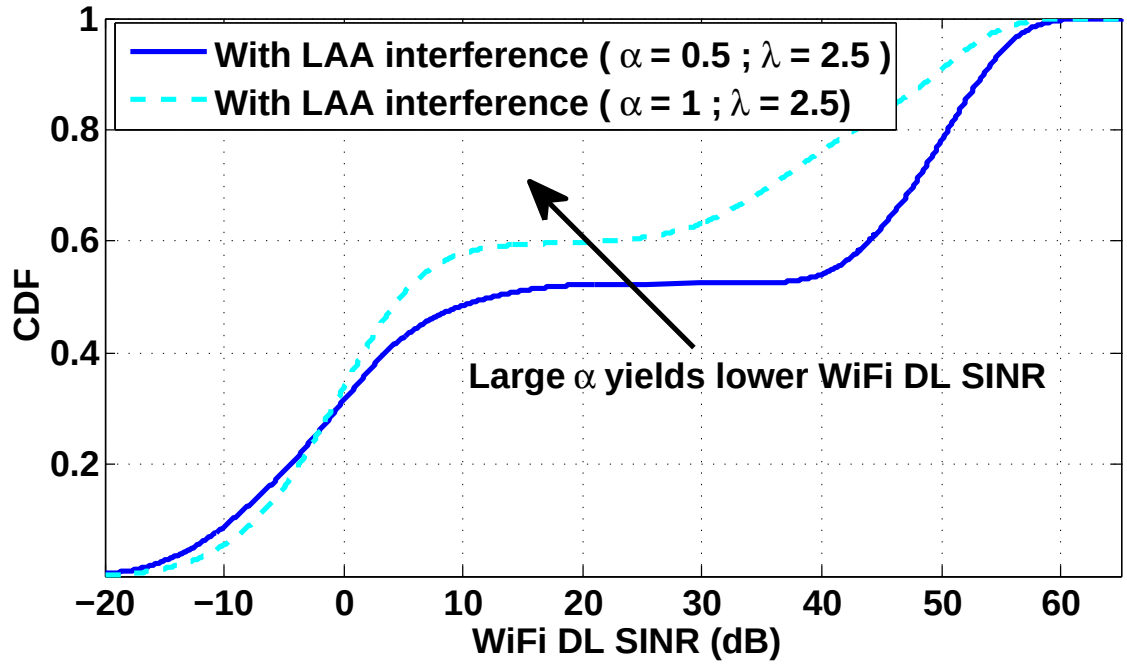

Figure 20: SINR distribution of WiFi DL with different α values.

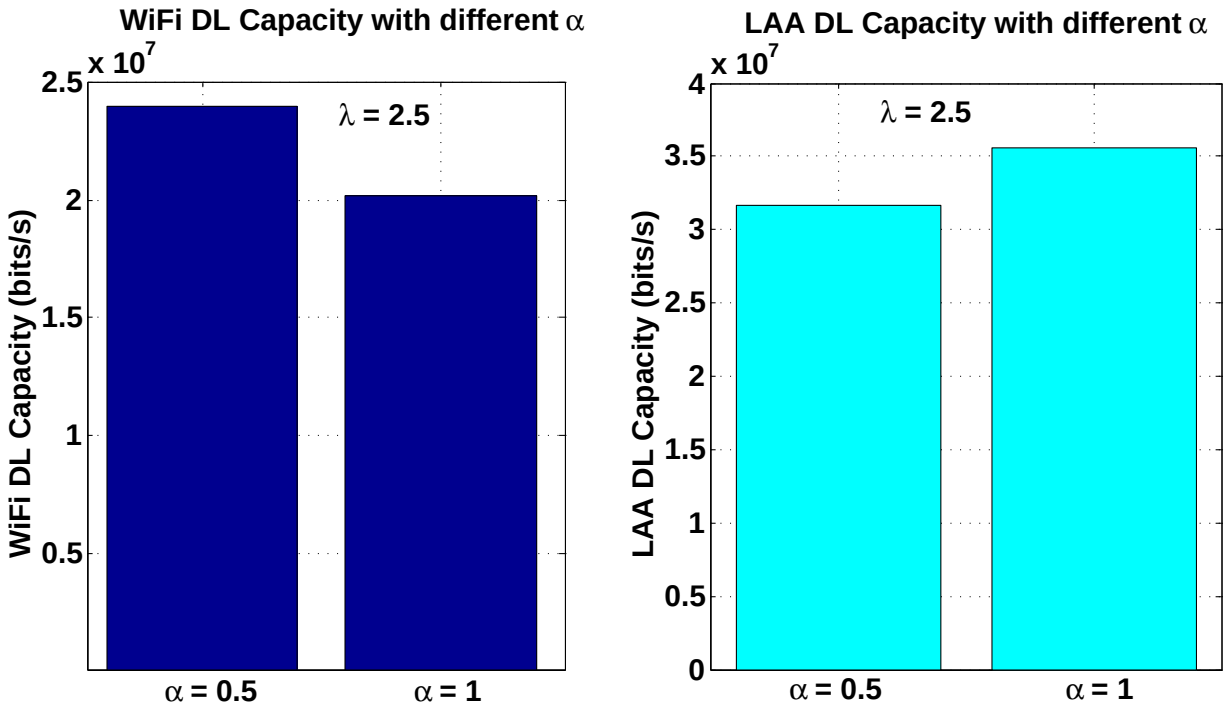

Figure 21: Average DL capacity (bits/s) of WiFi and LAA with different α values.

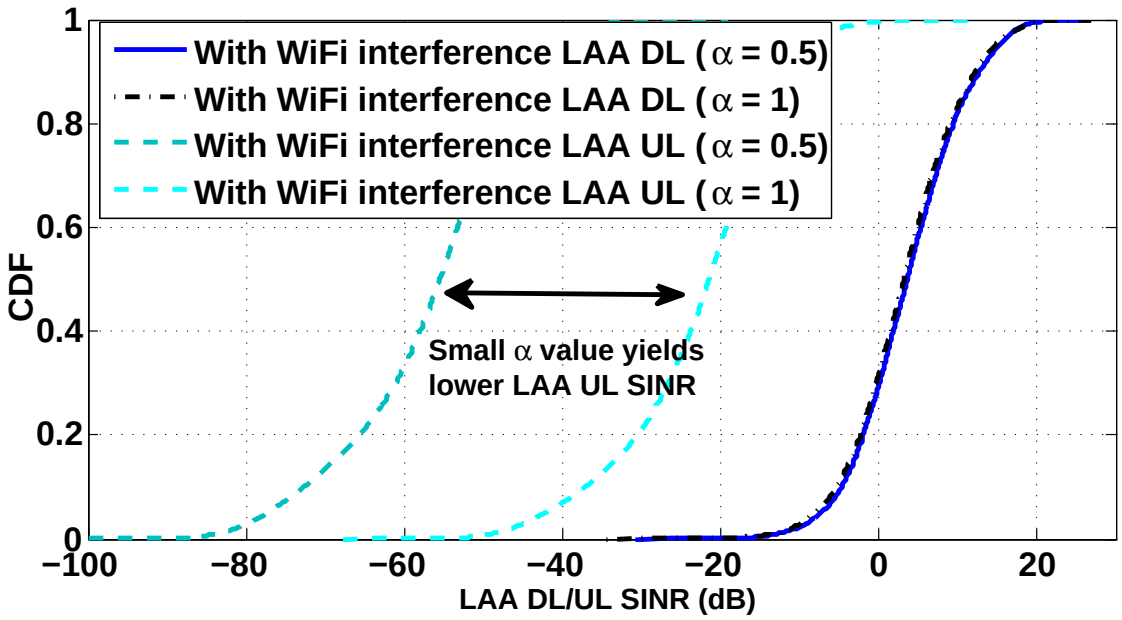

Figure 22: SINR distribution of LTE UL/DL with different α values.

degradation of WiFi is higher compared to LAA when they operate in the same frequency band. Nevertheless, by using different LTE TDD configurations (with more UL transmitting subframes), or LTE UL fractional power control mechanisms, it is possible to improve the WiFi performance, but with a slight degradation in LAA performance.

In the next section, a dynamic duty cycle selection mechanism for LTE transmission based on Q-Learning is presented to facilitate the simultaneous operation of WiFi and LTE in the unlicensed band.

CHAPTER IV

Reinforcement Learning for WiFi-LTE Coexistence

In this section, we introduce a reinforcement learning based dynamic duty cycle selection technique for LTE to facilitate WiFi-LAA simultaneous operation in the unlicensed spectrum. In particular, we use Q-Learning to dynamically configure transmission gaps in LAA periodically, based on its learnings from the environment. First, using a 3GPP-compliant simulation setting, we evaluate the system performance under different duty cycles of the transmission gaps. Then, the performance of Q-Learning based dynamic duty cycle selection technique is evaluated.

To achieve better coexistence performance evaluation with the proposed mechanism, we have explicitly taken in to consideration WiFi beacon transmission and in the next section a summary of the implemented beacon transmission model is provided.

4.1 WiFi Beacon Transmission

Beacon transmissions in WiFi networks are utilized by the WiFi STAs to detect WiFi APs. Reception of beacon frame is important since it contains information such as beacon interval, supported rates by the WiFi AP, and time stamp to synchronize with WiFi AP for transmission/reception of data to/from WiFi AP by a WiFi STA

Basic service set (BSS) is the basic building block of an 802.11n wireless local area network (WLAN) [1]. A BSS is formed when an association is created by STAs which are located within a certain coverage area. There are two types of BSS: 1) independent BSS (IBSS), and 2) infrastructure BSS (see Fig. 23). In IBSS, STAs communicate directly with

one another in an ad-hoc network. However, in infrastructure BSS, STAs associate with a central STA referred to as AP (WiFi AP is also an STA) which is dedicated to manage the BSS. The AP can be connected to a distribution system (DS) as shown in Fig. 23, through which AP is receiving data.

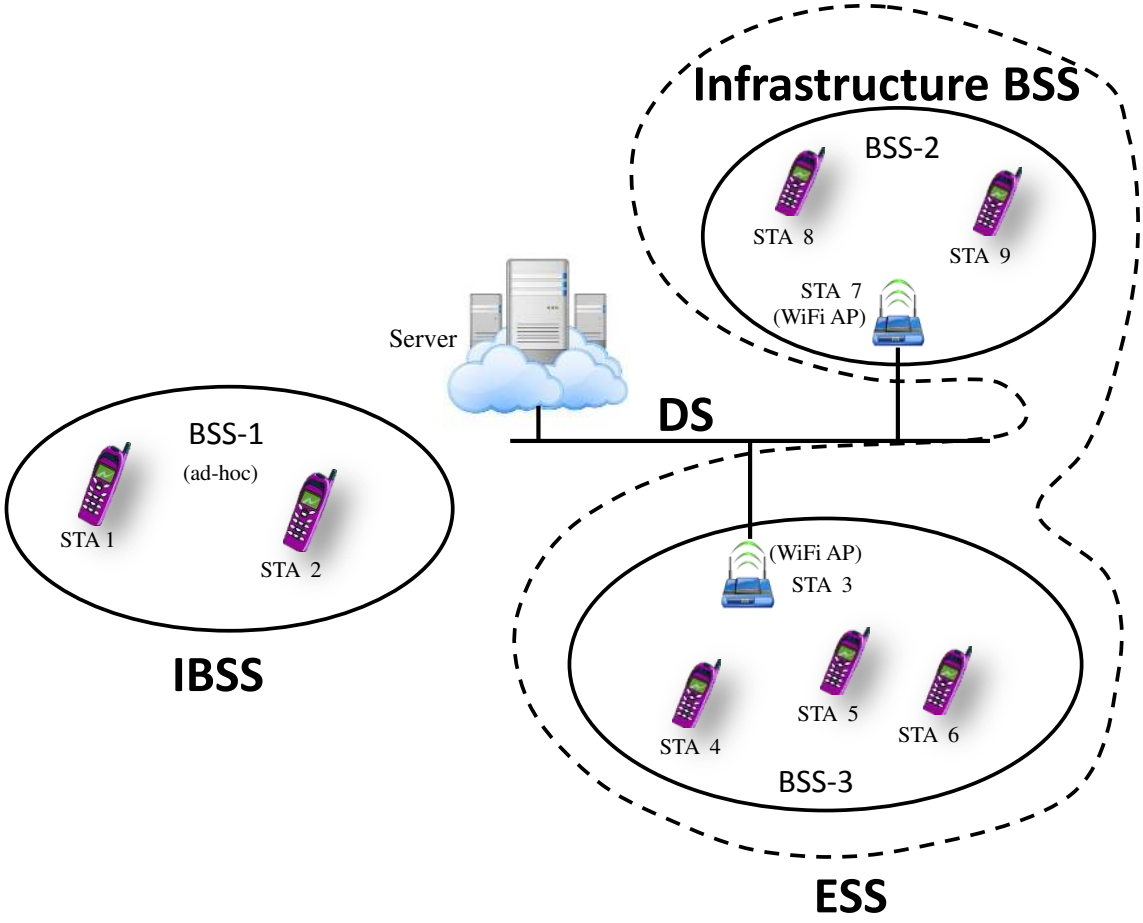

Figure 23: Structure of *Basic Service Set* (BSS). Two BSS types: 1) Infrastructure BSS 2) Independent BSS (IBSS). There can be several Infrastructure BSSs connected together via a *Distribution System* (DS). The BSSs interconnected by a DS is known as *Extended Service Set* (ESS).

The WiFi AP in an infrastructure BSS, periodically broadcasts beacon frames. The time period for beacon transmission is known as *target beacon transmission time* (TBTT). Beacon transmissions are utilized by the WiFi STAs to detect WiFi APs. There are two ways to associate with an infrastructure BSS : 1) *passive scanning*, and 2) *active scanning*.

In *passive scanning*, STA scans the channel and try to detect a beacon frame. If required, STA may switch to other available channels and continue on scanning. Once STA discovers an AP through its beacon frame, it may request for additional information, if required, using a *probe request/response* frame exchange. Beacon frame usually includes information such as the country code, maximum allowable transmit power, and the channel to be used for the regulatory domain, among other information [1]. On the other hand, in *active scanning*, STA transmits *probe request* frames on each of the channels it is seeking a BSS. For this *probe request*, an AP that receives the request will send a *probe response* frame, if some conditions are satisfied.

As shown in Fig. 24, in an infrastructure BSS with passive scanning, sometimes it is not possible to transmit beacon exactly at the TBTT by WiFi AP. This is because, WiFi AP has to wait till the completion of all the ongoing WiFi transmissions of STAs associated with that AP, before transmitting the beacon frame. STAs refrain from starting new WiFi transmissions when TBTT time is approaching. Before transmitting a beacon frame, WiFi AP waits for a time duration specified by the *point co-ordination function inter-frame space* (PIFS) to ensure medium is free. Successful reception of beacon frame is important because, without that it is not possible for an STA to transmit/receive data. In this thesis, we consider infrastructure BSS with passive scanning for WiFi transmission as explained here.

4.1.1 Beacon Frame

Beacon is a management medium access control (MAC) frame. Fig. 25 shows the beacon *physical protocol data unit* (PPDU) considered in the thesis. In that, *beacon payload* represents the MAC frame. Beacon frame is always transmitted using BPSK modulation with code rate of $1/2$.

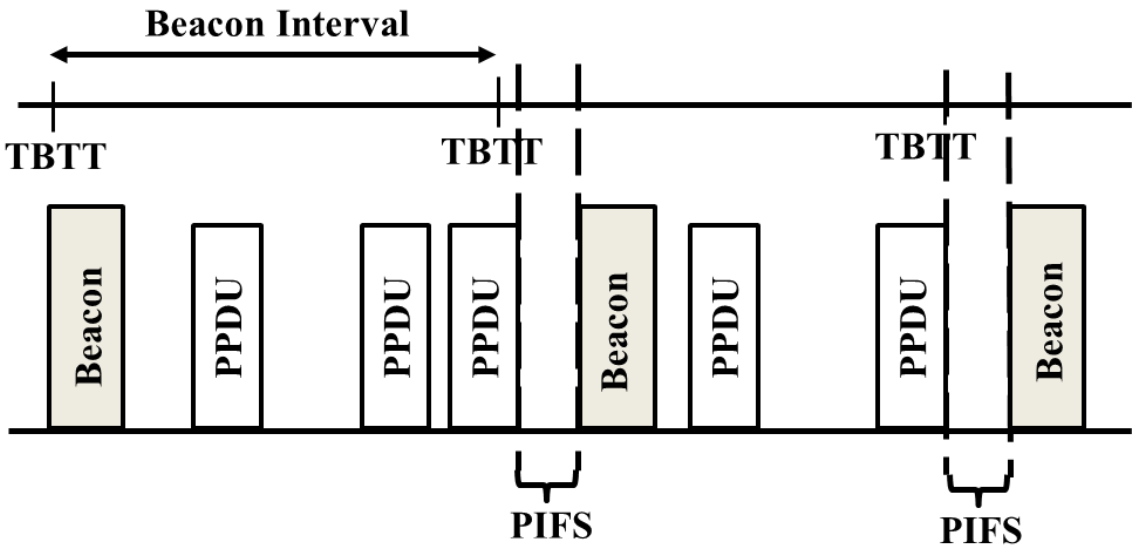

Figure 24: Beacon transmission

Figure 25: Beacon PPDU.

Modeling of Beacon Transmission

As PHY layer abstraction is used to calculate the capacity in WiFi and LTE transmissions, we implement following method to identify successful reception of a beacon PPDU (frame) at an STA.

First, to determine whether an *orthogonal frequency division multiplexing* (OFDM) symbol carrying a portion of the beacon PPDU was received at an STA, observed SINR of that OFDM symbol ($SINR_{\mathrm{B}}^{\mathrm{OFDM}}$) is compared against a threshold ($SINR^{\mathrm{Th}}$) as follows;

$$SINR_{\mathrm{B}}^{\mathrm{Beacon}} \geq SINR^{\mathrm{Th}} \tag{8}$$

If above (8) is satisfied, it is assumed that the information in that OFDM symbol was

properly received by the STA. The same detection mechanism is used by the STA for all the OFDM symbols belongs to a particular beacon PPDU. At the end of the beacon PPDU transmission, WiFi STA calculates erroneously received beacon PPDU bits by summing up bits in all the unsuccessfully received beacon OFDM symbols. Then, the ratio (ρ) between erroneously received bits to all the transmitted beacon bits (N_{B}) of the beacon PPDU is calculated as

$$\rho = \frac{N_{\mathrm{err}} \times N_{\mathrm{B}}^{\mathrm{OFDM}}}{N_{\mathrm{B}}}, \tag{9}$$

where N_{err} and $N_{\mathrm{B}}^{\mathrm{OFDM}}$ are the number of erroneously received beacon OFDM symbols and number of bits in a beacon OFDM symbol, respectively. The ratio in (9) is then compared with a predefined threshold for acceptable bit error ratio of a beacon PPDU and determines whether the beacon PPDU is successfully received at the WiFi STA.

4.2 Duty Cycle Implementation for LAA

To implement duty cycle based LAA transmission, we consider a TDD configuration as shown in Fig. 26. The rationale behind selecting this type of a TDD configuration is to keep the UL to DL sub frame ratio constant irrespective of the selected duty cycle. In particular, a sequence of four subframes are assumed always to consist of two DL subframes, one UL subframe and one guard subframe.

Four different duty cycles are considered with a transmission gap duty cycle period of 20 ms. As shown in Fig. 26, LTE transmits for x percentage of time from the allocated duty cycle period. For an example, if we consider 60% duty cycle, LTE will transmit for 12 ms out of 20 ms duty cycle period. When moving between adjacent duty cycles (i.e., from 20% to 40%), LTE transmission duration is increased/decreased with a granularity of 4 ms. As the subframe pattern gets repeated for every 4 ms, changing between duty cycles will add/remove block(s) of considered subframe pattern while keeping DL to UL

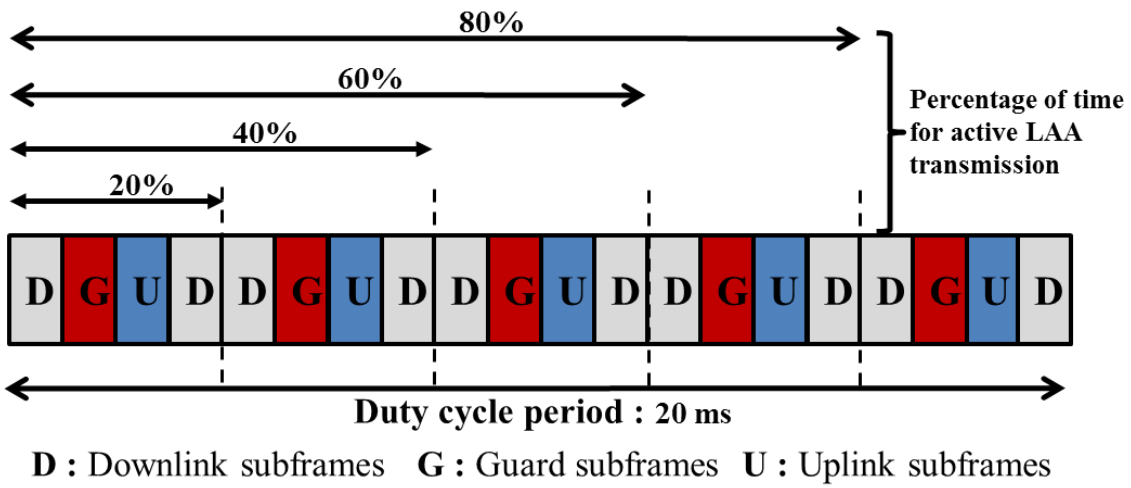

Figure 26: Proposed TDD configurations for LTE

subframe ratio constant.

4.3 Q-Learning Based Dynamic Duty Cycle Selection for LAA

In this section, we present Q-Learning based dynamic duty cycle selection algorithm for LAA transmission. Dynamic duty cycle selection is important since the network traffic is bursty in realistic systems. Hence, the proposed approach can help in enhancing LTE operation in the unlicensed spectrum while providing more opportunities for WiFi transmission. As proposed in [54], we consider a Q-Learning algorithm with ε-greedy policy. In that, a pre-defined target capacity value (C_{tar}) is set for LAA DL, and LAA BSs autonomously aim to operate at a capacity close to C_{tar} by dynamically adjusting their duty cycles.

When formulating the proposed Q-Learning algorithm, we consider set of LAA BSs ($\mathcal{B}$), as the players/agents of the multi-agent system. Each player $i \in \mathcal{B}$ has set of actions $\mathcal{A}_i = \{a_{i,1}, a_{i,2}, .., a_{i,|\mathcal{A}_i|}\}$ and states $\mathcal{S}_i = \{s_{i,1}, s_{i,2}, .., s_{i,|\mathcal{S}_i|}\}$ where $a_{i,j}$ and $s_{i,k}$ represents a possible action and a state of player i, respectively. In Q-Learning, each player $i \in \mathcal{B}$ keeps a Q-table with Q-values $Q_i(s_{i,j}, a_{i,k})$ for each state $s_{i,j} \in \mathcal{S}_i, 1 \leq j \leq |\mathcal{S}_i|$ and action $a_{i,k} \in \mathcal{A}, 1 \leq k \leq |\mathcal{A}_i|$ pair (see Fig. 27). This Q-value provides an estimate for future costs,

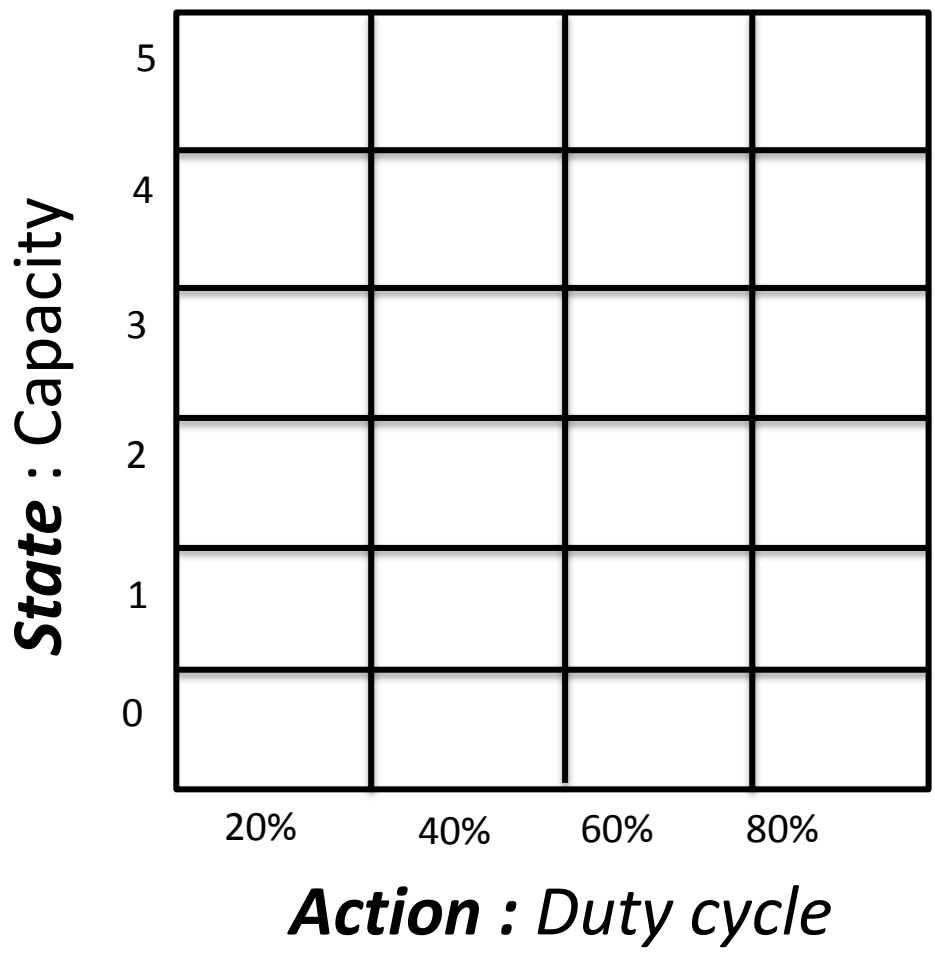

Figure 27: Q-Table maintained by each LAA BS.

if the player i selects the action $a_{i,k}$ when he is in the state $s_{i,j}$.

A player i in a particular state $s_{i,j}$, selects and deploys an action $a_{i,k}$. Then, based on the feedback from the environment, the player learns about the outcome of the deployed action $a_{i,k}$ in state $s_{i,j}$. This feedback is given as a cost value $c_i, i \in \mathcal{B}$, which determines the absolute difference between the achieved LAA DL capacity $C_{\text{LAA},i}, i \in \mathcal{B}$, during the previous duty cycle period and the target capacity C_{tar}. Using $C_{\text{LAA},i}$ new state of player i, $s_{i,l} \in \mathcal{S}_i, 1 \leq l \leq |\mathcal{S}_i|$ is also identified. Then, using the identified next state $s_{i,l}$ and calculated

cost value c_i, Q-value of the current state ($s_{i,j}$) and action ($a_{i,k}$) pair is updated as follows:

$$\begin{aligned} Q_i(s_{i,j},a_{i,k}) \leftarrow (1-\alpha)Q_i(s_{i,j},a_{i,k}) \\ +\alpha\big[c_i+\gamma\min_{a_{i,m}}Q_i(s_{i,l},a_{i,m})\big], \end{aligned} \tag{10}$$

where, α, γ are the learning rate and discount factor respectively. As can be seen from (10), the new Q-value of the current state/action pair depends on the current Q-value of that state/action pair ($Q_i(s_{i,j},a_{i,k})$), calculated cost (c_i), and minimum Q-value of the identified next state, $\min_{a_{i,m}}Q_i(s_{i,l},a_{i,m})$. In this way, learning is achieved in the proposed algorithm.

The learning rate α $(0 \leq \alpha \leq 1)$ determines how quickly the learning can occur. If α is too small, it will take long time to complete the learning process, while if it is too high, algorithm might not converge. The discount factor $\gamma\,(0 \leq \gamma \leq 1)$ controls the value placed on the future costs. If γ is too small, learning will not depend on future costs much and immediate costs are optimized. On the other hand, if it is too high, learning will count on future costs heavily. Through a careful selection of these two parameters, it is possible to effectively control the learning process of the proposed Q-Learning approach.

Once the Q-value of the current state ($s_{i,j}$) and action ($a_{i,k}$) pair is updated, an action $a_{i,m} \in \mathcal{A}_i, 1 \leq m \leq |\mathcal{A}_i|$ is selected for the next state $s_{i,l}$. A random number $r \in \mathcal{U}(0,1)$ is generated first and compared against the ε-greedy parameter which is usually a very small value $(0.01 \leq \varepsilon \leq 0.05)$. If r is smaller than the ε-greedy parameter, an action will be selected randomly. Otherwise, the action with the minimum Q-value, ($a_{i,m} = \text{argmin}_{a_{i,m}}Q_i(s_{i,l},a_{i,m})$) in the identified next state ($s_{i,l}$), is selected. The ε-greedy parameter allows selecting an action in an exploratory way, and ensures that all state/action pairs will be explored as the number of trials goes to infinity. The proposed Q-Learning algorithm is summarized in Algorithm 1.

Algorithm 1 Q-Learning for duty cycle selection of LAA BS $i \in \mathcal{B}$

Initialize:
for each $s_{i,j} \in \mathcal{S}_i, 1 \leq j \leq |\mathcal{S}_i|$, $a_{i,k} \in \mathcal{A}, 1 \leq k \leq |\mathcal{A}_i|$ **do**
    Initialize the Q-value representation mechanism $Q_i(s_{i,j}, a_{i,k})$
end for
Evaluate the starting state $s = s_{i,j} \in \mathcal{S}_i, 1 \leq j \leq |\mathcal{S}_i|$
Learning:
loop
    Generate a random number $r \in \mathcal{U}(0,1)$
    if $(r < \varepsilon)$ **then**
        Select action randomly
    else
        Select the action $a_{i,m} \in \mathcal{A}_i$ characterized by the min(Q-value)
    end if
    Execute $a_{i,m}$
    Receive an immediate capacity $C_{\text{LAA},i}$ and cost c_i
    Observe the next state $s_{i,l} \in \mathcal{S}_i, 1 \leq l \leq |\mathcal{S}_i|$
    Update the Q-table entry as follows:
        $Q_i(s_{i,j}, a_{i,k}) \leftarrow (1-\alpha) Q_i(s_{i,j}, a_{i,k})$
        $+\alpha[c_i + \gamma \min_{a_{i,m}} Q_i(s_{i,l}, a_{i,m})$
    $s = s_{i,l}$
end loop

Without any loss of generality, we consider that the action, state and cost definitions in the proposed algorithm are defined as follows.

• **Action:** $\mathcal{A}_i = \{20\%, 40\%, 60\%, 80\%\}$.

• **State:**

$$s_{i,j} = \begin{cases} 0, & C_{\text{LAA},i} < 1\,\text{Mbps} \\ 1, & 1\,\text{Mbps} \leq C_{\text{LAA},i} < 10\,\text{Mbps} \\ 2, & 10\,\text{Mbps} \leq C_{\text{LAA},i} < 20\,\text{Mbps} \\ 3, & 20\,\text{Mbps} \leq C_{\text{LAA},i} < 30\,\text{Mbps} \\ 4, & 30\,\text{Mbps} \leq C_{\text{LAA},i} < 40\,\text{Mbps} \\ 5, & C_{\text{LAA},i} \geq 40\,\text{Mbps} \end{cases}. \tag{11}$$

• **Cost:**

$$c_i = |C_{\text{tar}} - C_{\text{LAA},i}|, \tag{12}$$

where $C_{\text{LAA},i}$ is given by,

$$C_{\text{LAA},i} = \frac{N^{DC}_{\text{Bits},i}}{T^{DC}_{\text{Tx},i} + T^{DC}_{\text{Wait},i}}. \tag{13}$$

In (13), for LAA BS $i \in \mathcal{B}$, $N^{DC}_{\text{Bits},i}$ represents number of bits successfully transmitted during the previous duty cycle period. $T^{DC}_{\text{Tx},i}$ and $T^{DC}_{\text{Wait},i}$ are the total transmitting time and the waiting time due to silent subframe allocation[1] respectively, during the previous duty cycle period.

4.4 Simulation Results Discussion - Q-Learning Based WiFi-LTE Coexistence

In simulations, we consider a two layer cell layout as shown in Fig. 11. Each layer consists of $M = 7$ cells. There are $N = 10$ WiFi STAs (LAA UEs) associated with each WiFi AP (LAA BS). WiFi STAs (LAA UEs) move within the cell with a speed of 3 km/h. WiFi and LAA traffic arrival rates, $\lambda_{\text{WiFi}} = \lambda_{\text{LAA}} = 2.5$, are considered in all the simulations. LTE and WiFi 802.11n MAC and PHY layers are implemented as described in section III. Round robin user scheduling is considered in LAA DL transmission and only one user is scheduled during each transmission time interval (TTI). The LAA UEs report the observed DL SINR value during a DL transmission to the LAA BS, which is then used by the LAA BS to determine the number of RBs to be allocated for the next DL transmission. Based on the number of LAA UE requests for UL transmission during one subframe, bandwidth is equally divided between them. All the configuration parameters used for LAA in simulations are given in Table 3.

[1] LAA BS $i \in \mathcal{B}$ has data to schedule in DL. However, due to silent subframe allocation, it has to wait.

Table 4: WiFi beacon model parameters.

Parameter	Value
Beacon Interval	100 ms
Beacon OFDM symbol detection threshold	10 dB
Beacon error ratio threshold	15

For WiFi, CSMA/CA is implemented with *enhanced distributed channel access* (EDCA) and *clear channel assessment* (CCA) [51]. WiFi beacon transmission is implemented, as discussed in Section 4.1, for realistic performance evaluations. All the STAs (including WiFi AP) having data in their respective queues can compete for the channel access when no transmission is going on in the cell. The WiFi STA (or the WiFi AP) sensing the channel to be idle and having the shortest back-off time will gain the access to the channel if it has received the most recent beacon successfully. If the beacon has not been received successfully, the WiFi STA can not initiate any transmission or reception. All the configuration parameters used for WiFi in simulations are summarized in Table 2 and Table 4. In all performance evaluations, we focus on the performance of center cell in both WiFi and LAA cell layouts.

4.4.1 Performance Analysis with WiFi Beacon Transmission

We evaluate WiFi and LAA performance with WiFi beacon transmission considering TDD configuration 2. Fig. 28 shows WiFi and LAA DL average capacity, with/without beacon transmission. There is an improvement in LAA DL capacity and degradation in WiFi capacity when beacon transmission exists. The reason for this is that, when a STA misses a beacon, it cannot transmit or receive until a beacon is received successfully. Therefore, when WiFi beacon transmission exists, number of simultaneous WiFi data transmissions reduces. As a result, WiFi interference on LAA DL reduces and LAA DL capacity improves. Moreover, missing a beacon at a WiFi STA further delays WiFi transmission. This will result in increasing WiFi waiting time, and hence reduces WiFi capacity.

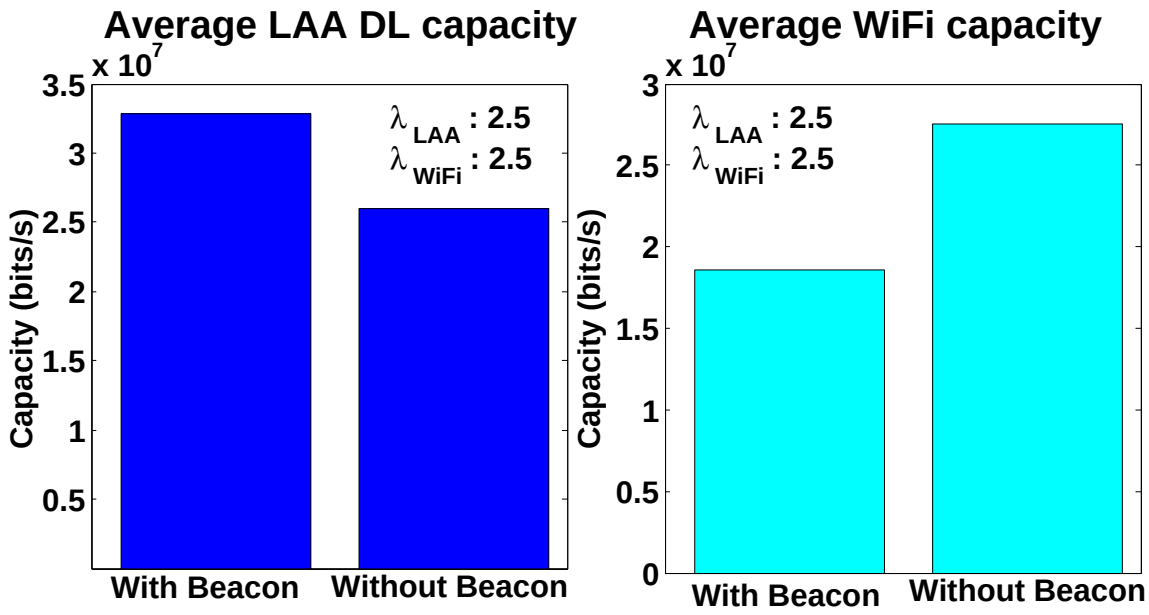

Figure 28: WiFi and LAA DL capacity variation with/without beacon transmission.

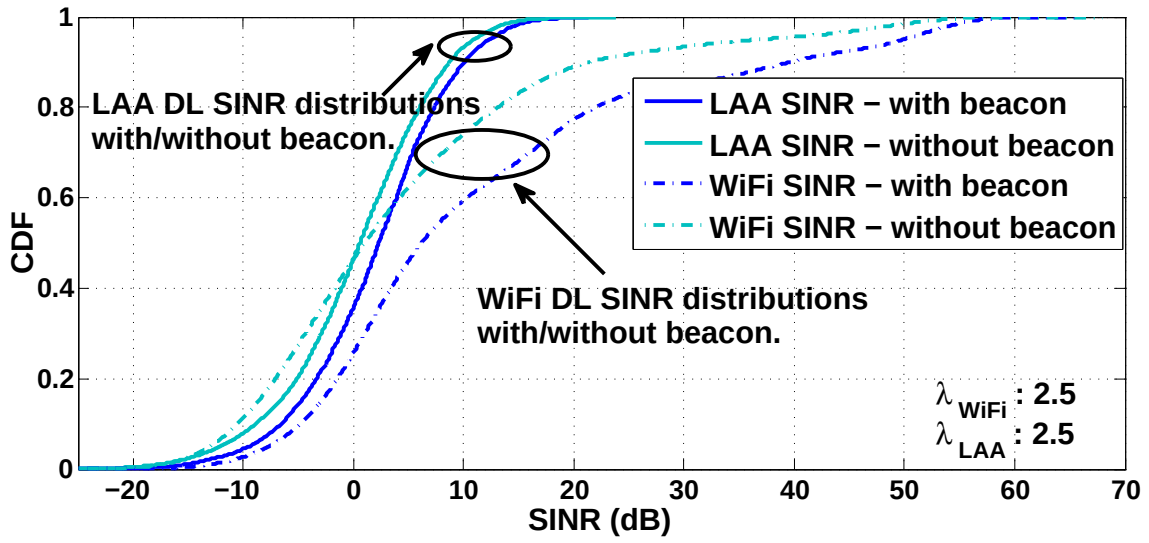

Figure 29: WiFi/LAA DL SINR distributions with/without WiFi beacon transmission.

Fig. 29 shows SINR distributions at WiFi and LAA DL with/without WiFi beacon transmission. The LAA DL SINR improves with WiFi beacon transmission, since the WiFi interference on LAA reduces due to the reduction of the number of simultaneous WiFi transmissions. WiFi SINR distribution with/without WiFi beacon transmission is also shown in Fig. 29, where an improvement in WiFi SINR can be seen with beacon transmission. This is due to the lower WiFi interference with the reduced number of simultaneous WiFi transmissions. Note here that the SINR is captured during WiFi transmission and this does not help much for improving WiFi capacity, as waiting time for WiFi increases with missed beacons. That is why we see a capacity reduction in Fig. 28 for WiFi, when WiFi beacon transmission exists.

4.4.2 Performance Analysis with Different LAA Duty Cycles

In this section, we evaluate WiFi and LAA performance under four different duty cycles considering TDD configuration presented in Section 4.2. Fig. 30 shows WiFi and LAA capacity variation under different LAA duty cycles. While the WiFi capacity decreases with larger LAA duty cycles, the LAA capacity increases. This is because, with larger LAA duty cycles, LAA interference on WiFi increases and as a result WiFi capacity decreases. On the other hand, LAA capacity increases with higher duty cycles due to more transmission opportunities. Note here that the rate of WiFi capacity degradation reduces with LAA duty cycle. The reason for this observation is, with higher duty cycles, number of simultaneous WiFi transmissions reduces. Therefore, WiFi interference is reduced, decreasing the WiFi capacity degradation rate.

Fig. 31 captures WiFi DL SINR distributions with four different duty cycles. The results show that WiFi SINR degrades with higher LAA duty cycles. This is because, interference coming from LAA increases with higher LAA duty cycles. A step like behavior can be observed in the WiFi DL SINR distribution. This is due to the difference in LTE DL and UL interference on WiFi as explained in section 3.9.1.

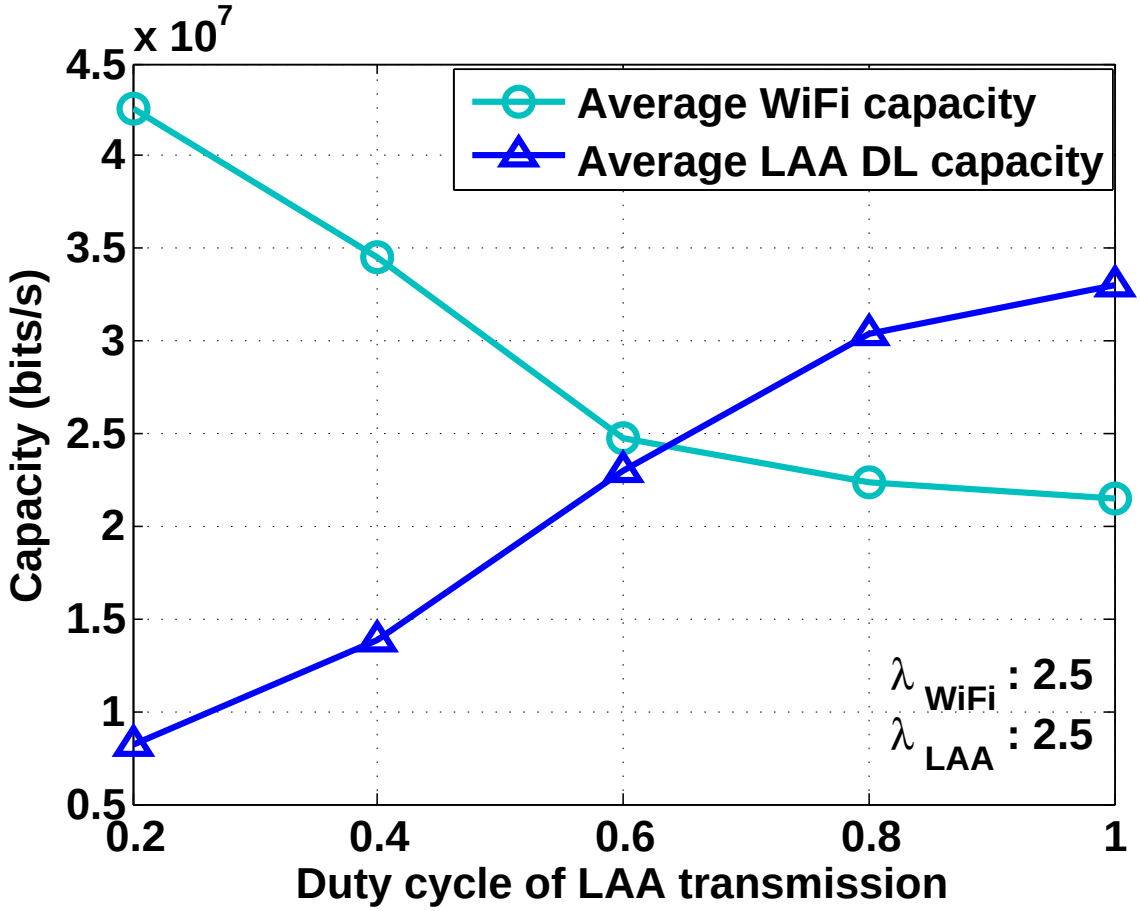

Figure 30: Average LAA DL and WiFi capacity variations with different duty cycles for duty cycle period of 20 ms.

From Fig. 32, we can observe LAA DL SINR distribution with four different duty cycles. In that, LAA SINR improves with larger duty cycle. This is because of the lower WiFi interference experienced due to the reduced number of simultaneous WiFi transmissions.

4.4.3 Performance Analysis with Q-Learning Based Dynamic Duty Cycle Selection for LAA

In this section, we evaluate the performance of the proposed Q-Learning based dynamic duty cycle selection technique. For simulations, we consider $\alpha = 0.5$, $\gamma = 0.9$, $\varepsilon = 0.03$, and $C_{\text{tar}} = 30$ Mbps with the TDD configuration introduced in Section 4.2.

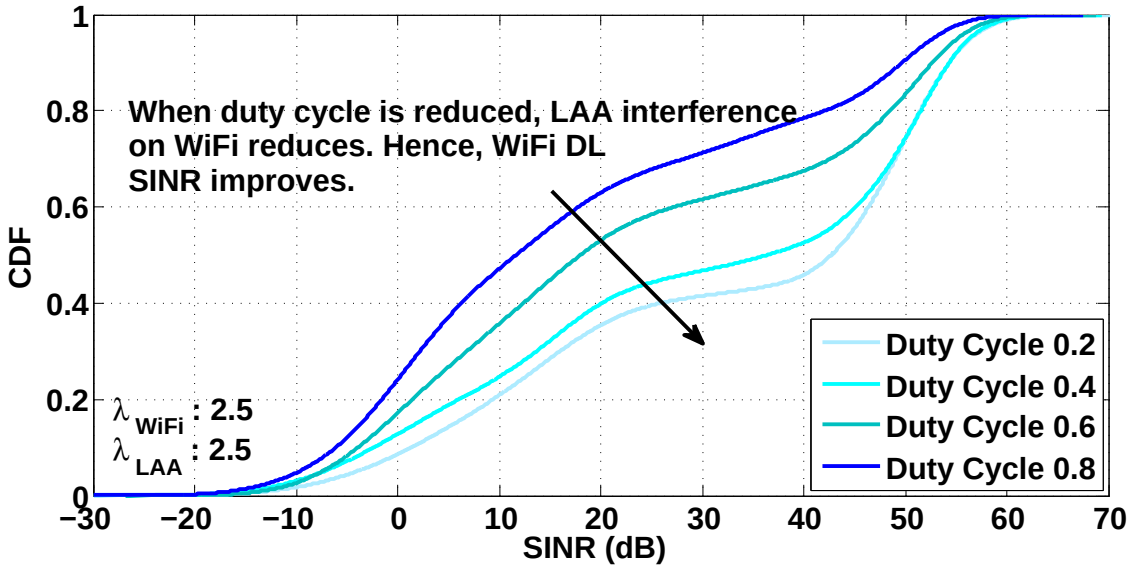

Figure 31: WiFi DL SINR distribution with different LAA duty cycles.

Fig. 33 shows the aggregate capacity variation (WiFi and LAA DL) with different duty cycles and Q-Learning based dynamic duty cycle selection technique. The Q-Learning based dynamic duty cycle selection technique provides highest total capacity when compared with fixed duty cycle and full LAA transmission scenarios. The reason for this capacity gain is that, as the LAA BSs dynamically adjust their operating duty cycles based on the bursty traffic arrival given the capacity constraint C_{tar}, WiFi gets fair amount of transmission opportunities. As the medium sensing procedure in WiFi is one of the main barriers which prevents WiFi from achieving higher capacities, the proposed technique provides a solution to overcome that problem. According to Fig. 33, the next highest total capacity is achieved when operating without any transmission gaps. However, as can be seen from Fig. 30, achievable WiFi capacity is the lowest (21.45 Mbps) in this case, whereas with Q-Learning based approach, WiFi capacity of 39.7 Mbps could be achieved while keeping LAA capacity around $C_{\text{tar}} = 30$ Mbps.

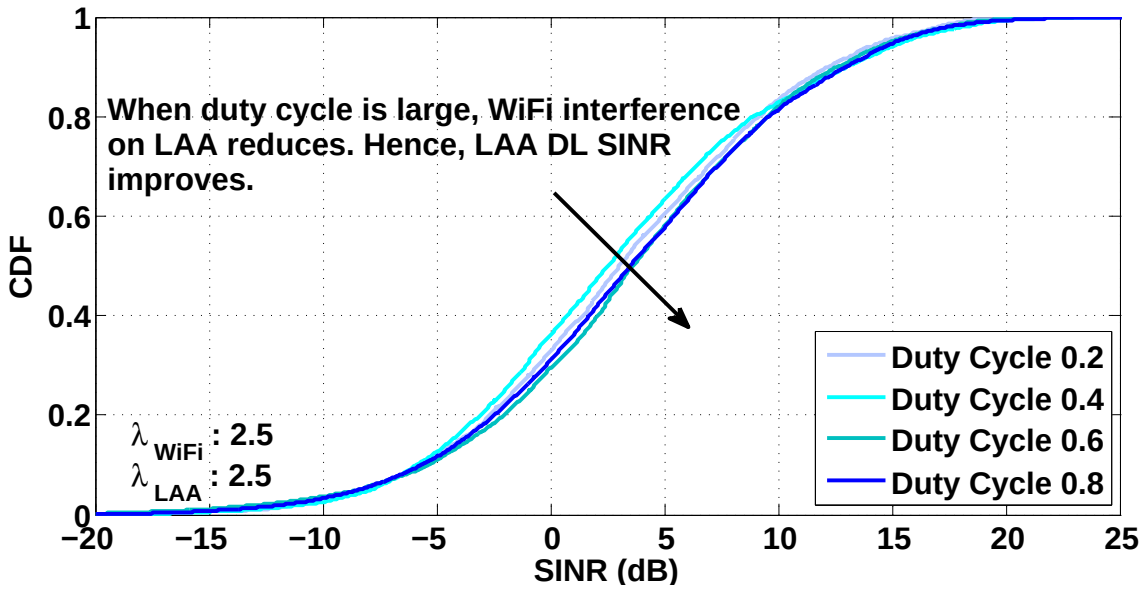

Figure 32: LAA DL SINR distribution with different LAA duty cycles.

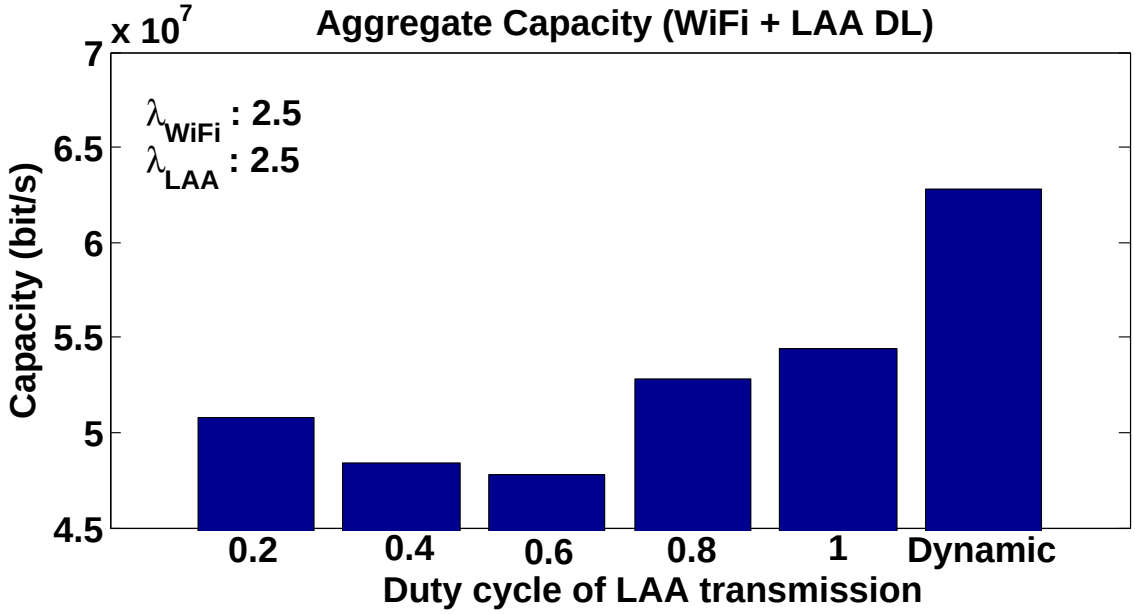

Figure 33: Aggregate capacity (WiFi + LAA DL) variation

CHAPTER V

Concluding Remarks

In this thesis we studied WiFi and LAA coexistence performance under three different scenarios, considering a multi layer cell layout. Simulation results show that performance degradation of WiFi is higher compared to LAA when they operate in the same frequency band. Nevertheless, by using different LTE TDD configurations (with more UL transmitting subframes), or LTE UL fractional power control mechanisms, it is possible to improve the WiFi performance, but with a slight degradation in LAA performance.

Then, to facilitate this coexistence, we have proposed a Q-Learning based dynamic duty cycle selection approach in which periodic transmission gaps are configured by LAA, so as to effectively coexist with WiFi systems in the unlicensed spectrum. First, we evaluate WiFi and LAA performance with a fixed value of the transmission gap. Then, the overall system performance with the proposed Q-Learning based dynamic duty cycle selection approach is evaluated. Simulation results show that the proposed dynamic duty cycle selection approach for LAA can effectively enhance the overall capacity performance.

REFERENCES

[1] E. Perahia and R. Stacey, *Next Generation Wireless LANs: Throughput, Robustness, and Reliability in 802.11n*. Cambridge Univ. Press, 2008.

[2] Ericsson, "LTE Licensed Assisted Access," Jan. 2015. [Online]. Available: http://www.ericsson.com/res/thecompany/docs/press/media_kits/ericsson-license-assisted-access-laa-january-2015.pdf

[3] "Evolved Universal Terrestrial Radio Access (E-UTRA); Further advancements for E-UTRA physical layer aspects (Release 9)," Tech. Rep. 3GPP TR36.814, V9.0.0, Mar. 2010.

[4] Cisco, "Cisco Visual Networking Index: Global Mobile Data Traffic Forecast Update, 2013−2018," Feb. 2014, White Paper.

[5] Qualcomm, "The 1000x mobile data challenge: More small cells, more spectrum, higher efficiency," Nov. 2013.

[6] B. Obama. (2010, Jun.) Presidential Memorandum: Unleashing the Wireless Broadband Revolution. [Online]. Available: http://www.whitehouse.gov/the-press-office/presidential-memorandum-unleashing-wireless-broadband-revolution

[7] National Science Foundation. (2010, Aug.) Workshop on ENHANCING ACCESS TO THE RADIO SPECTRUM. [Online]. Available: http://www.nsf.gov/mps/ast/nsf_ears_workshop_2010_final_report.pdf

[8] "Study on Licensed-Assisted Access using LTE," 3GPP Study Item - RP-141397, Edinburgh, Scotland, Sep. 2014.

[9] W. Yuan, X. Wang, and J. P. M. G. Linnartz, "A Coexistence Model of IEEE 802.15.4 and IEEE 802.11b/g," in *Proc. IEEE Symp. on Commun. Vehic. Techno. in the Benelux*, Nov. 2007, pp. 1–5.

[10] S. Zacharias, T. Newe, S. O'Keeffe, and E. Lewis, "Coexistence measurements and analysis of IEEE 802.15.4 with Wi-Fi and bluetooth for vehicle networks," in *Proc. IEEE Conf. Telecommun. (ITST)*, Nov. 2012.

[11] N. Golmie, N. Chevrollier, and O. Rebala, "Bluetooth and WLAN coexistence: challenges and solutions," *IEEE Wireless Communi.*, vol. 10, no. 6, pp. 22–29, Dec 2003.

[12] L. Angrisani, M. Bertocco, D. Fortin, and A. Sona, "Experimental Study of Coexistence Issues Between IEEE 802.11b and IEEE 802.15.4 Wireless Networks," *IEEE Trans. Instrumentation and Measurement*, vol. 57, no. 8, pp. 1514–1523, Aug 2008.

[13] S. Pollin, I. Tan, B. Hodge, C. Chun, and A. Bahai, "Harmful Coexistence Between 802.15.4 and 802.11: A Measurement-based Study," in *Proc Int. Conf. on Cognitive Radio Oriented Wireless Networks and Communi.*, May 2008, pp. 1–6.

[14] B. H. Jung, J. W. Chong, C. Jung, S. M. Kim, and D. K. Sung, "Interference Mediation for Coexistence of WLAN and Zigbee Networks," in *Proc. IEEE Int. Symp. on Personal, Indoor and Mobile Radio Communi.*, Sept 2008, pp. 1–5.

[15] Q. Liu, X. Li, W. Xu, and D. Zhang, "Empirical Analysis of Zigbee and WiFi Coexistence," in *Proc. ,Int. Conf. Innovative Design and Manufacturing (ICIDM)*, Aug 2014, pp. 117–122.

[16] S. Mishra, R. Brodersen, S. Brink, and R. Mahadevappa, "Detect and Avoid: An Ultra-Wideband/WiMAX Coexistence Mechanism," *IEEE Commun. Mag.*, vol. 45, no. 6, pp. 68–75, Jun. 2007.

[17] P. Rathod, A. Karandikar, and A. Sahoo, "Facilitating Non-collocated coexistence for WiFi and 4G wireless networks," in *Proc. IEEE Conf. Local Comp. Netw. (LCN)*, Oct. 2012, pp. 1–9.

[18] M. E. Şahin, İsmail Güvenc, and H. Arslan, "An iterative interference cancellation method for co-channel multicarrier and narrowband systems," *Physical Commun.*, vol. 4, no. 1, pp. 13 – 25, 2011.

[19] M. B. Çelebi, İsmail Güvenç, H. Arslan, and K. A. Qaraqe, "Interference suppression for the LTE uplink," *Physical Commun.*, vol. 9, no. 0, pp. 23 – 44, 2013.

[20] B. Han, Y. Liang, L. Huo, X. Zhang, and D. Yang, "Coexistence of Downlink High-Speed Railway Communication System with TDD-LTE Cellular Communication System," in *Proc IEEE Vehicular Technol. Conf. (VTC Spring)*, May 2012, pp. 1–6.

[21] L. Polak, O. Kaller, L. Klozar, and J. Prokopec, "Exploring and Measuring the Co-Existence between LTE and DVB-T2-Lite Services," in *Proc. Int. Conf. on Telecommuni. and Signal Processing (TSP)*, Jul. 2013, pp. 316–320.

[22] Z. Meng, Y. Hai, F. Yulin, and C. Yongyu, "Coexistence Studies on the Interference Performance between Mobile Satellite System and LTE Network," *China Communications*, vol. 10, no. 7, pp. 1–11, July 2013.

[23] Huawei, "U-LTE: Unlicensed Spectrum Utilization of LTE," 2014. [Online]. Available: www.huawei.com/ilink/en/download/HW_327803

[24] Broadcom Corporation, "Discussion on Licensed Assited LTE," 3GPP RAN1 standard contribution - RWS-140022, Sophia Antipolis, France, Jun. 2014.

[25] Texas Instruments, "LTE Operation in Unlicensed Spectrum," 3GPP RAN1 standard contribution - RWS-140012, Sophia Antipolis, France, Jun. 2014.

[26] "Review of Regulatory Requirements for Unlicensed Spectrum," 3GPP RP-140054, Fukuoka, Japan, Sep. 2014.

[27] NOKIA, "LTE in Unlicensed Spectrum : European Regulation and Co-Existence Considerations," 3GPP RAN1 standard contribution - RWS-14002, Sophia Antipolis, France, Jun. 2014.

[28] "Summary of a workshop on LTE in Unlicensed Spectrum," Tech. Rep. 3GPP TSG RAN Meeting 63, Fukuoka, Japan, Mar. 2014.

[29] HiSilicon, "Scenarios, spectrum considerations and preliminary assessment results of U-LTE," 3GPP RAN1 standard contribution - RWS-140026, Sophia Antipolis, France, Jun. 2014.

[30] InterDigital, "A Look at the Requirements for LTE in the Unlicensed Spectrum," 3GPP RAN1 standard contribution - RWS-140006, Sophia Antipolis, France, Jun. 2014.

[31] Alcatel Lucent, "On the Standardisation of LTE in Unlicensed Spectrum," 3GPP RAN1 standard contribution - RWS-140014, Sophia Antipolis, France, Jun. 2014.

[32] AT&T, "Assited Access for LTE," 3GPP RAN1 standard contribution - RWS-140003, Sophia Antipolis, France, Jun. 2014.

[33] NTT DOCOMO, "Views on LAA for Unlicensed Spectrum - Scenarios and Initial Evaluation Results," 3GPP RAN1 standard contribution - RWS-140026, Sophia Antipolis, France, Jun. 2014.

[34] SONY, "Requirements and Coexistence Topics for LTE-U," 3GPP RAN1 standard contribution - RWS-140010, Sophia Antipolis, France, Jun. 2014.

[35] ZTE, "Discussion on LTE in Unlicensed Spectrum," 3GPP RAN1 standard contribution - RWS-140021, Sophia Antipolis, France, Jun. 2014.

[36] Samsung, "Performance Evaluation of LTE in Unlicensed Spectrum," 3GPP RAN1 standard contribution - RWS-140016, Sophia Antipolis, France, Jun. 2014.

[37] Hitachi, "Hitachi perspectives on LTE-U," 3GPP RAN1 standard contribution - RWS-140017, Sophia Antipolis, France, Jun. 2014.

[38] CATT, "Considerations on LTE-U in Rel-13," 3GPP RAN1 standard contribution - RWS-140019, Sophia Antipolis, France, Jun. 2014.

[39] A. Cavalcante, E. Almeida, R. Vieira, F. Chaves, R. Paiva, F. Abinader, S. Choudhury, E. Tuomaala, and K. Doppler, "Performance Evaluation of LTE and Wi-Fi Coexistence in Unlicensed Bands," in *Proc. IEEE Vehi. Technol. Conf. (VTC)*, June 2013, pp. 1–6.

[40] Qualcomm, "Extending LTE Advanced to unlicensed spectrum," Dec. 2013, White Paper.

[41] ——, "Extending the benefits of LTE Advanced to Unlicensed Spectrum," Apr. 2014.

[42] ——, "LTE in Unlicensed Spectrum : Harmonious Coexistence with WiFi," Jun. 2014, White Paper.

[43] Intel, "LTE Sysyem Deployment and Performance in Unlicensed Bands," Tech Talk at IEEE ComSoc Event on LTE-U, Nov. 2014.

[44] M. Beluri, E. Bala, Y. Dai, R. Di Girolamo, M. Freda, J. Gauvreau, S. Laughlin, D. Purkayastha, and A. Touag, "Mechanisms for LTE Coexistence in TV White Space," in *Proc. IEEE Int. Symp. on Dynamic Spectrum Access Networks (DYSPAN)*, Oct. 2012, pp. 317–326.

[45] R. Ratasuk, M. Uusitalo, N. Mangalvedhe, A. Sorri, S. Iraji, C. Wijting, and A. Ghosh, "License-exempt LTE deployment in heterogeneous network," in *Proc. Int. Symp. Wireless Commun. Sys. (ISWCS)*, Aug. 2012.

[46] E. Almeida, A. Cavalcante, R. Paiva, F. Chaves, F. Abinader, R. Vieira, S. Choudhury, E. Tuomaala, and K. Doppler, "Enabling LTE/WiFi Coexistence by LTE blank subframe allocation," in *Proc. IEEE Inter. Conf. on Commun. (ICC)*, Jun. 2013, pp. 5083–5088.

[47] CableLabs, "Cable Labs perspective on LTE-U Coexistence with Wi-Fi and Operational Modes for LTE-U," 3GPP RAN1 standard contribution - RWS-140004, Sophia Antipolis, France, Jun. 2014.

[48] F. Chaves, E. Almeida, R. Vieira, A. Cavalcante, F. Abinader, S. Choudhury, and K. Doppler, "LTE UL Power Control for the Improvement of LTE/Wi-Fi Coexistence," in *Proc. IEEE Vehic. Technol. Conf. (VTC)*, Sep. 2013, pp. 1–6.

[49] Dongning Guo, "LTE in Unlicensed Spectrum," Communication Theory Workshop, Curacao, May. 2014.

[50] NOKIA, "Nokia LTE for Unlicensed Spectrum," 2014, White Paper.

[51] N. Rupasinghe and I. Güvenç, "Licensed-Assisted Access for WiFi-LTE Coexistence in the Unlicensed Spectrum," in *Proc. IEEE Global Telecommun. Conf. (GLOBECOM) Workshops - Emerging Technologies for 5G Wireless Cellular Networks*, Dec. 2014.

[52] ——, "Reinforcement Learning for Licensed-Assisted Access of LTE in the Unlicensed Spectrum," in *Proc. IEEE Wireless Commun. Networking Conf. (WCNC) (Submitted)*, Mar. 2015.

[53] S. Sesia, I. Toufik, and M. Baker, *LTE : From Theory to Practice, 2nd Edition*. John Wiley and Sons Ltd, 2011.

[54] M. Simsek, A. Czylwik, A. Galindo Serrano, and L. Giupponi, "Improved Decentralized Q-learning Algorithm for Interference Reduction in LTE-femtocells," in *Proc. Wireless Adv.*, Jun. 2011, pp. 138–143.